KARADENİZ TECHNICAL UNIVERSITY
THE GRADUATE SCHOOL OF NATURAL AND APPLIED SCIENCES

DEPARTMENT OF MECHANICAL ENGINEERING

COOLING ANALYSIS OF A LONG DISTANCE BUS CABIN USING EXPERIMENTAL AND NUMERICAL METHODS

MASTER THESIS

Zeki Mert BARUT

JULY 2019
TRABZON

KARADENİZ TECHNICAL UNIVERSITY

THE GRADUATE SCHOOL OF NATURAL AND APPLIED SCIENCES

DEPARTMENT OF MECHANICAL ENGINEERING

COOLING ANALYSIS OF A LONG DISTANCE BUS CABIN USING EXPERIMENTAL AND NUMERICAL METHODS

Zeki Mert BARUT

This thesis is accepted to give the degree of

"MASTER OF SCIENCE"

By

The Graduate School of Natural and Applied Sciences at
Karadeniz Technical University

The Date of Submission : **20 / 05 /2019**

The Date of Examination : **08 / 07 /2019**

Supervisor : **Prof. Dr. Orhan AYDIN**

Trabzon 2019

KARADENİZ TECHNICAL UNIVERSITY

THE GRADUATE SCHOOL OF NATURAL AND APPLIED SCIENCES

DEPARTMENT OF MECHANICAL ENGINEERING

Zeki Mert BARUT

COOLING ANALYSIS OF A LONG DISTANCE BUS CABIN USING EXPERIMENTAL AND NUMERICAL METHODS

Has been accepted as a thesis of

MASTER OF SCIENCE

after the Examination by the Jury Assigned by the Administrative Board of the Graduate School of Natural and Applied Sciences with the Decision Number 1807 dated 14 / 06 / 2019

Approved By

Chairman : Prof. Dr. Orhan AYDIN

Member : Prof. Dr. Mehmet Emin ARICI

Member : Prof. Dr. Adnan MİDİLLİ

Prof. Dr. Asim KADIOĞLU

Director of Graduate School

FOREWORD

This study, which is fuelled by never ending curiosity of understanding the nature to improve every system around me as an engineer, significantly contributed my CFD skills and brought me a comprehensive understanding of how to approach an industrial problem which can lead to a benefit to a commercial enterprise. Yet, I see this effort as a droplet on quenching my eternal flame of curiosity and my passion on improving industrial systems.

I would like to express my deepest gratitude to my supervisor Prof. Dr. Orhan Aydın and my co-advisor Assist. Prof. Dr. Özgür Ekici for their extensive guidance, support and contributions during the overall development of the study. Secondly, I would like to thank to my directors in the R&D Center of MAN Truck & Bus Ankara Plant, Mr. Ertuğrul Çifçi and Mr. Hüseyin Çavdar for the technical and financial support, to my colleagues Ms. Müge Sincer, Mr. Kemal Çağın Akar, Mr. Ali Kemal Koyuncu, Mr. Halil İbrahim İnan, Mr. Oğuz Ünal, Mr. Çağatayhan Kılıç and Mr. Umut Aktaş, for their generous contributions during the preparation of the analysis geometry, Mr. Kemal Edip Yıldırım and Mr. Marius Hellmold for their valuable advices abroad and Mr. Gökhan Güney for the inspiration. I also acknowledge the generous support Mr. Ümit Ulusoy and Mr. Hakan Dedealemdaroğlu during the experimental data collection, extensive contributions of Mr. Kaan Peneklioğlu and Mr. Alper Yıldırım from NUMESYS on establishing the numerical model and valuable consultancy of Dr. Murat Eray Korkmaz during the submission procedures. Without them, this study would not be deemed much successful.

Last but not least, I am indebted to every single member of my family, notably my mother, my father, my sister and my aunt for their never ending support and my beloved wife for being all I have.

Zeki Mert BARUT

Ankara 2019

ETHICAL DECLARATION

In this thesis study named “Cooling Analysis of a Long Distance Bus Cabin using Experimental and Numerical Methods”, I hereby declare that I completed the whole study from the beginning on the supervision of my advisor Prof. Dr. Orhan Aydın and my co-advisor Assist. Prof. Dr. Özgür Ekici, collected all the data / samples, executed all the experiments / analysis studies in the relevant laboratories, referred every information gathered from external sources in the context and in the references, followed the scientific research ethical conduct and acknowledged any legal circumstances otherwise. 08/07/2019

Zeki Mert BARUT

TABLE OF CONTENTS

Page No

Master's Thesis

SUMMARY

Cooling Analysis of a Long Distance Bus Cabin using Experimental and Numerical Methods

Zeki Mert BARUT

Karadeniz Technical University
The Graduate School of Natural and Applied Sciences
Mechanical Engineering Graduate Program
Supervisor: Prof. Orhan AYDIN
Co-Advisor: Assist. Prof. Özgür EKİCİ
2019, 52 Pages

Vehicle manufacturers are on a continuous challenge of increasing the fuel efficiency of their vehicles. Considering the energy withdrawn, the air conditioning unit stands as an important component to be investigated for increasing the overall efficiency of vehicles. In this study, the computational fluid dynamics (CFD) model of a long distance bus cabin is numerically validated by the experimental data obtained from a full scale bus tested in a climatic chamber. In the numerical methods, a transient analysis is conducted using ANSYS Fluent® numerical solver with employing realizable k-ε method and boussinesq approximation under the considerations of time-dependent temperature boundary conditions at the inlets, convection boundary conditions at the window and adiabatic walls. The results, however, indicate that the consideration of heat absorbed by the seat materials, convective heat transfer and conductive heat transfer from the walls are of great importance in the validation of a cabin cooling procedure under transient conditions.

Key Words: Temperature distribution, Cabin cooling, Computational fluid dynamics (CFD) analysis

Yüksek Lisans Tezi

ÖZET

Bir Uzun Mesafe Seyahat Otobüsü Kabininin Soğutulmasının Deneysel ve Nümerik Yöntemlerle Analizi

Zeki Mert BARUT

Karadeniz Teknik Üniversitesi
Fen Bilimleri Enstitüsü
Makina Mühendisliği Anabilim Dalı
Danışman: Prof. Dr. Orhan AYDIN
İkinci Danışman: Dr. Öğretim Üyesi Özgür EKİCİ
2019, 52 Sayfa

Taşıt üreticileri, ürünlerinin yakıt verimliliğini artırmak için süregelen bir mücadele içerisindedir. Taşıtlarda klima sistemleri, aracın yürütülmesi için harcanan enerjiden sonra ikinci büyük enerji tüketicisi durumundadır. Bu durum, taşıtların toplam verimliliğinin artırılması için klima sistemlerini incelenmesi gereken önemli bir bileşen olarak karşımıza çıkarmaktadır. Bu çalışmada bir uzun mesafe seyahat otobüsünün hesaplamalı akışkanlar dinamiği (HAD) modeli, tam ölçekli bir otobüsün kabininin sıcaklık kontrollü bir klimatik odada soğutulması ile elde edilen zaman bağımlı deneysel veriler kullanılarak doğrulanmıştır. Sayısal yöntemlerde kullanılan modelde hava girişlerinde zaman bağımlı sıcaklık ve sabit hava hızı sınır şartı, camda taşınım ısı transferi sınır şartı ve duvarlarda adyabatik sınır şartı uygulanmış bir HAD modeli, *realizable k-ε* metodu ve *boussinesq* yaklaşımının kullanıldığı ANSYS Fluent® çözücüsü ile zaman bağımlı olarak çözülmüştür. Çalışma sonucunda, bir kabinin zamana bağlı soğutma analizinde koltukların soğurduğu ısı ile duvarlarda iletim ve taşınım yoluyla ısı transferinin göz önünde bulundurulmasının önemli bir rol oynadığı gözlenmiştir.

Anahtar Kelimeler: Sıcaklık dağılımı, Kabin soğutması, Hesaplamalı akışkanlar dinamiği (HAD) analizi

TABLE OF FIGURES

Page No

LIST OF TABLES

Page No

LIST OF ABBREVIATIONS

CFD	: Computational Fluid Dynamics
A/C	: Air Conditioning
HVAC	: Heating Ventilation and Air Conditioning
SIMPLE	: Semi Implicit Method for Pressure Linkage Equations
RNG	: Re-normalization Group
RANS	: Reynolds–averaged Navier-Stokes
BC	: Boundary Condition
SU	: Service Unit
R	: Roof
avg	: Average
pbns	: Pressure-based Navier-Stokes
rke	: Realizable k-ε
exp	: Experimental
num	: Numerical

NOMENCLATURE

c_p	specific heat capacity (J/kgK)
F	body force (N)
g	gravitational acceleration (m/s²)
h	heat transfer coefficient (W/m²K)
k	Turbulent kinetic energy (m²/s²)
k	thermal conductivity (W/mK)
Nu	Nusselt number
p	pressure (N/m²)
P	mean pressure (N/m²)
Pr	Prandtl number
q	heat flux (W/m²)
R	equivalent thermal resistance
Re	Reynolds number
T	absolute temperature (K)
t	time (s)
τ	shear stress (N/m²)
U	mean velocity (m/s)
u	velocity (m/s)
u_τ	friction velocity (m/s)
$\overline{u_i' u_j'}$	Reynolds stress tensor
y	vertical distance from wall (m)
y^+	dimensionless wall distance

Greek Letters

β	thermal expansion coefficient
ε	turbulent dissipation rate (m²/s³)
μ	dynamic viscosity (kg/ms)

ν	kinematic viscosity (m^2/s)
∇	gradient operator
ρ	density (kg/m^3)
σ_k	turbulent Prandtl number for turbulent kinetic energy
σ_ε	turbulent Prandtl number for turbulent dissipation rate
τ	shear stress

Subscript

$_0$	initial
ais	aisle
cond	conduction
conv	convection
ext	external
s	surface
win	window
∞	ambient

Superscript

$^\circ$	degree
$^+$	plus
‘	fluctuating

1. INTRODUCTION

1.1. Motivation and Significance of the Study

Buses are considered as one of the most efficient vehicles for passenger transport for the last century, with the accessibility and reasonable transport costs they provide to passengers. Today, an average long distance bus (often referred to as a “coach” or a “touring bus”) can transfer up to 60 people for an average of 1300 kilometres in a single journey by consuming approximately 400 litres of diesel fuel.

Vehicle manufacturers are on a continuous challenge of increasing the fuel efficiency of the vehicles they produce. An internal combustion engine loses 64 to 69 percent of the total energy to the thermal losses due to the thermodynamic nature of the internal combustion and 4 to 7 percent of the power to the internal friction of the mechanical components. Apart from the A/C compressor load, an additional 2% of the energy is withdrawn by the auxiliary units such as climate control fans, seat heaters and defrosters. Only 20 to 30 per cent of the energy can be delivered to the wheels [1]. This makes the air conditioning systems the second largest energy consumers of a motor vehicle after driving itself [2, 3].

Any modifications made on the bus air-conditioning unit which might create a considerable effect on the overall fuel efficiency of the vehicle or on the passengers’ comfort often requires expensive and time consuming testing and validation activities. Today, the costs of an experiment made in a full scale wind tunnel varies between 0,5 and 1 €/second. This in turn motivates vehicle manufacturers to search for methods to avoid the number of field tests or experiments made in the wind tunnels or climatic chambers.

Nevertheless it will never replace either pure experiment or pure theory, computational fluid dynamics (CFD) stands as a “third approach” since 1960s and helping engineers to interpret and understand the results of the theory and experiment. [4]. As soon as the theory, simulations and limited number of experimental data are combined, this method is proven to be successful and is acknowledged as a modern tool by the designers [5]. This makes the CFD tools a very attractive low-cost and time efficient alternative to develop new products or improving the current ones.

According to the ASHRAE, air conditioning is the science of controlling the temperature, humidity, motion and cleanliness of the air within an enclosure. In a vehicle,

air conditioning means controlled and comfortable environment in the passenger cabin during summer and winter, i.e., control of temperature (for cooling or heating), control of humidity (decrease or increase), control of air circulation and ventilation (amount of air flow and fresh intake vs. partial or full recirculation), and cleaning of the air from odor, pollutants, dust, pollen, etc. before entering the cabin [6].

ASHRAE Standard 55 defines thermal comfort as "that state of mind which expresses satisfaction with the thermal environment" and prescribes 3ºC for the vertical air temperature difference between head and ankle level [7]. Other studies set this limit up to 6ºC [8].

Air conditioning units used in the buses are closed circuit systems and consist of at least a compressor, an evaporator, a condenser and an expansion valve. The conditioned air is supplied to the passengers through the two air ducts positioned along the cabin and the openings on these ducts.

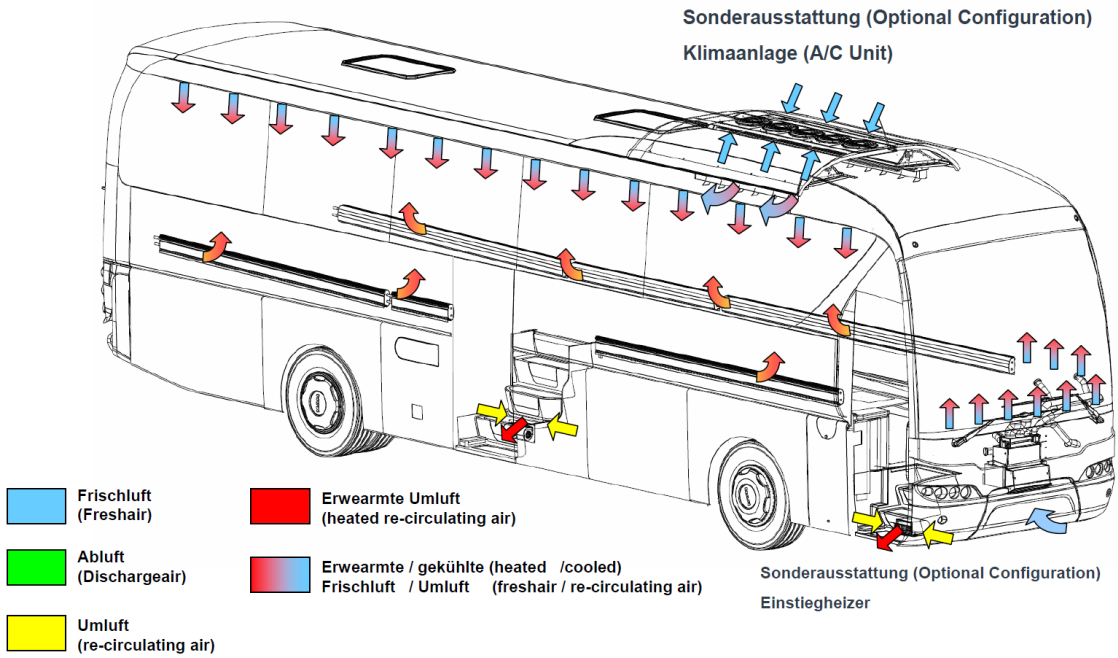

Figure 1. Air ventilation system of Neoplan Tourliner (MAN Truck & Bus AG).

In the refrigerant cycle, only the compressor, evaporators, condenser and the expansion valve is used. For the heating cycle, the main devices are the convectors which lies in the bottom of the two sides of the cabin, supplied with hot water which is heated by

the excess heat of the engine. For the heating of the bus, there is also an auxiliary heater which supplies heat to the cabin by directly consuming diesel fuel, which is kept out of the context of this study.

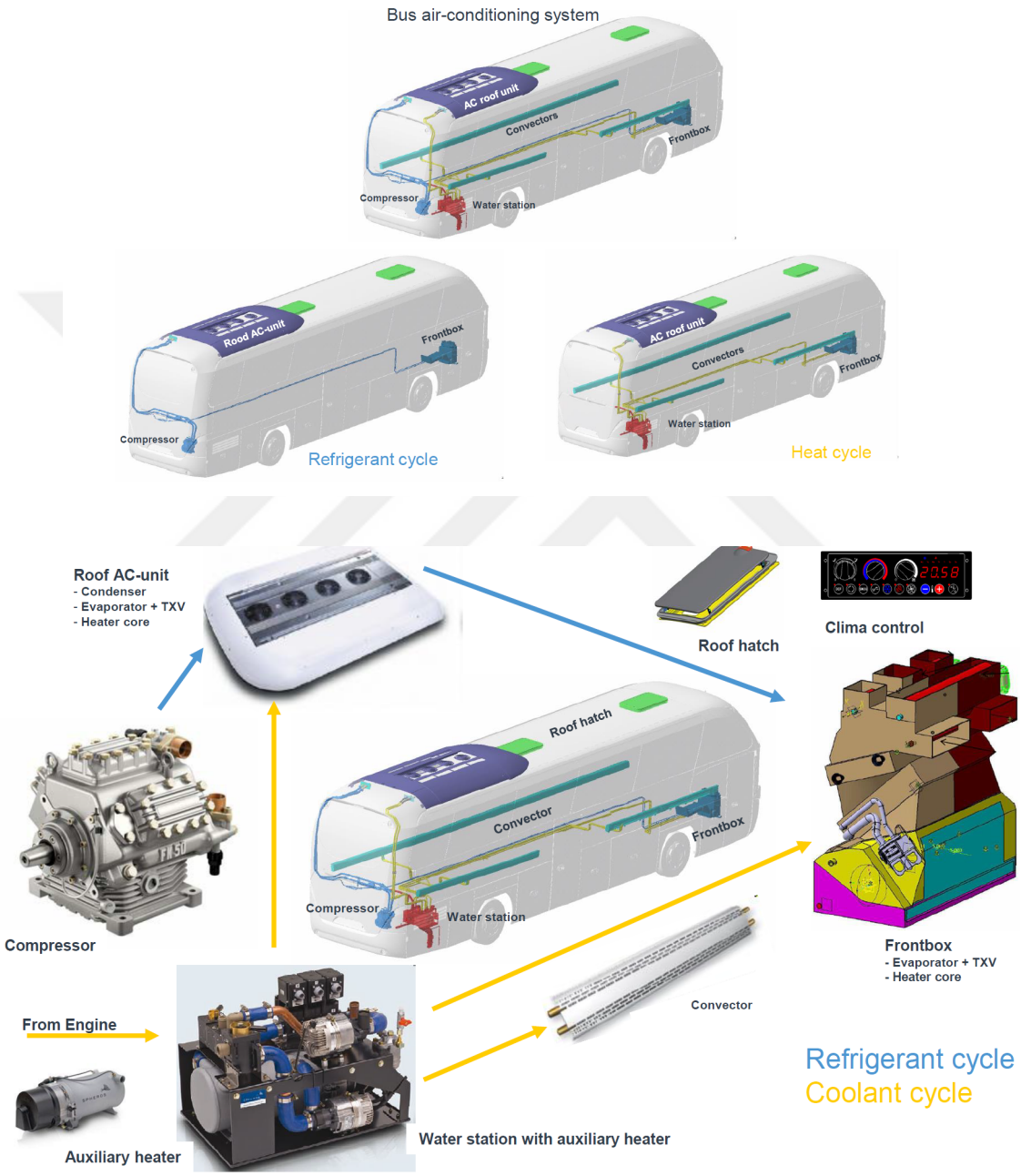

Figure 2. Components of the bus air conditioning system (MAN Truck & Bus AG).

1.2. Literature Review

There has been several studies which analyse the cabin environments in various types of vehicles by the use of CFD methods with the aim of increasing thermal comfort and energy efficiency. Types of the vehicles analysed and analysis methods used in the selected studies are listed in Table 1.

Table 1. Studies focused on thermal analysis of vehicle cabins

	Vehicle	Process	Time	Numerical Solver	Cells	Turbulence Model	Algorithm
Güney, 2016	Coach	Heating	Transient	Fluent	430k, Tetrahedral	RNG k-ε	SIMPLE / B-Force Weighted
Sevilgen, 2010	Car	Heating & cooling	Transient	Fluent	1M, Hexcore	RNG k-ε	Simple / Standard
Doğan, 2011	Truck	Cooling	Steady	Fluent	4,1 M, Tetrahedral	Standard k-ε	***
Şahin, 2018	Helicopter	Cooling	Steady	Fluent	4,5 M, Polyhedral	Standard k-ε + Boussinesq	***
Paulke et al., 2013	City bus	Cooling	Steady	THESEUS-FE	51k, Tetrahedral	***	***
Zhu et al., 2010	City bus	Heating	Steady	Star-CD	1 M, Tetrahedral	Standard k-ε	SIMPLE
Yıldırım et al., 2018	City bus	Cooling	Steady	-	-	-	-
Pala, 2014	Coach	Heating	Transient	MATLAB	-	-	-
You et al., 2018	Aircraft	Heating	Steady	Fluent	***	RNG k-ε + standart k-ω	SIMPLE / PRESTO!
Dehne et al., 2017	Car	Heating & Cooling	Steady	OpenFOAM	10 M, Hexahedral	k-Ω SST + Boussinesq	***
Petrone et al., 2008	Coach	Heating	Steady	COMSOL	360k Tetrahedral	Standard k-ε	***

***: not defined

Güney [9] studied the air flow and temperature distribution during the heating of a coach bus cabin. The study includes the creation of a CFD model of the half cabin section of a coach and validation of the model using experimental methods in order to investigate the thermal comfort of the passengers. The CFD model consists of a grid structure having 600k tetrahedral elements generated inside a cabin geometry created using ANSYS Design Modeler® solved by ANSYS Fluent® solver with the consideration of adiabatic walls and natural convection inside the cabin using the "Boussinesq approximation" with the experimentally obtained boundary conditions into the system. The transient analysis of the cabin model has been conducted using SIMPLE Algorithm and several turbulence models including RNG k-ε, realizable k-ε and standard k-ω.

Sevilgen [10] analysed the thermal comfort parameters during both the heating and cooling process of a passenger vehicle by creating a CFD model of a full cabin and validating the model with comparing the numerical and experimental methods. The study includes the analysis of temperature and velocity distribution inside the cabin having two manikins on the front seats having different temperatures on different faces with the consideration of radiation and convection heat transfer between the cabin and its surroundings. The cabin model having 1 million hexcore elements is created using Gambit software and the transient analysis of the cabin model was conducted using ANSYS Fluent solver with SIMPLE Algorithm and RNG k-ε turbulence model.

Doğan [11] created a CFD model of a truck cabin to examine the velocity and temperature distribution in occupant compartment of a heavy commercial truck and validated the model using experimental methods. The study, which involves the convection, conduction and radiation effects inside and outside of the cabin, consists of creating a 3D model of the truck with two passengers prepared and simplified using CATIA®, generating a mesh structure which has 4,1 million tetrahedral elements created using HyperMesh® and Harpoon® Mesher and solving the model using ANSYS Fluent in steady-state conditions.

Şahin [12] investigated the thermal comfort level of the passengers in a passenger transportation helicopter by creating a CFD model with 12 passengers having a total of 4,8 million polyhedral mesh elements and solving the model using ANSYS Fluent with standard k-ε model for turbulence modelling, Boussinesq approximation for natural convection and wall thickness approximation for conduction considerations. The study is mainly focused on determining the air velocity since the air flow in the vicinity of the faces of passengers is the primary concern.

Paulke, et al. [13] investigated the HVAC system of a city bus under solar loads by creating an extended simulation model which can also be employed for simulating passenger thermal comfort. The CFD model of the whole city bus consists of 51.800 solid elements which is solved under the considerations of internal and external convection, solar radiation, heat conduction through walls and windows and engine compartment. The solution obtained using THESEUS-FE® is validated by comparing the results from simplified energy balance model (SEBM) -an internal tool using in MAN Truck & Bus considering energy balances for the bus cabin- and the results obtained using Mollier Diagram which both indicate that the net power of the HVAC system needed to maintain the internal air temperature to a constant of 20°C is 16 kW.

Zhu et al. [14] examined the micro-environmental conditions in public transportation buses by developing and experimentally validating a CFD model. The grid structure created using Gridgen® which has 1 million tetrahedral elements is solved using Star-CD software with under the employment of standard k-ε turbulence model and implicit SIMPLE algorithm. The solution is validated with the experimental data obtained from the measurements from an actual bus. The results indicate that the air velocities among the cabin are generally dispersed as smaller than 0,3 m/s which nearly satisfies the comfort standards, however, the simulated results and measured results did not show a great agreement in the areas with low air velocities and low Reynolds number, due to the utilization of standard wall function used in the model.

Yıldırım et al. [15] assessed the temperature asymmetry inside a city bus cabin due to the solar exposure in order to counteracting these non-homogeneous temperature distribution through targeted zonal air conditioning. The measurements made with the infrared cameras exposed a temperature difference up to 12°C on the window surfaces and 5°C on the seat surfaces between the sun-exposed and shady sides of a bus which indicates the necessity of a zonal climatic system for passenger comfort. Additionally, the study indicates a potential of energy savings up to 27 kWh due to the cooling upon the zonal passenger density in the cabin.

Pala [16] investigated the thermal comfort parameters in bus design by means of an experimental work including a full performance heating test of a vehicle, a calculation for determining the skin temperatures and mathematical calculations conducted by means of a code written on MATLAB®. In the experimental work, a full scale bus is tested under the GBK (Gütegemeinschaft BusKomfort e.V.) standards which requires the temperature of the

bus cabin to reach +20°C from -20°C within 90 minutes. In the numerical work, a MATLAB code is prepared based on Transient Energy Balance Model in which the governing energy balance and heat transfer equations and mathematical relations for sweating and respiration are stated.

You et al. [17] proposed and validated a new and innovative ventilation system for airliner cabin by means of conducting experimental measurements on a mock-up of a cabin section inside an air-controlled room and using these experimental measurements as input parameters to a CFD model of the cabin section. The CFD model is solved using ANSYS Fluent with a hybrid turbulence model which takes the advantage of the robustness of RNG k-ε model in the bulk air regions and superiority of the SST k-ω model in the near wall regions. The SIMPLE Algorithm is employed for coupling pressure and velocity and PRESTO! scheme for discretizing pressure. Nevertheless the study mainly focuses on the velocity distribution and air flow rate changes which emphasizes the advantages of the innovative system proposed, temperature distribution among the cabin was also investigated. In conclusion, the proposed system is found that it has a good potential in contaminant removal and acceptable in the means of thermal comfort.

Dehne et al. [18] compared three new ventilation concepts with the objective of improving thermal comfort of the passengers and energy efficiency of the future vehicles. The study consists of an experiment which includes thermal testing of a mock-up of a generic car cabin that is capable of simulating the 4 different ventilation concepts under winter, spring/fall and summer conditions and a CFD simulation which is validated with the experimental data allowing a comprehensive understanding into the 3D Flow structures. The grid structure of the passenger vehicle created using StarCCM+® which consists of nearly 10 million hexahedral elements is solved using OpenFOAM® with the considerations of thermal boundary conditions for walls, Boussinesq approximation for capturing the natural convection and k-Ω/SST model for capturing the turbulences inside the cabin. The results indicate that even though none of the ventilation systems was able to provide comfort conditions according to ISO 14505-2 standart in winter conditions, vertical ventilation provide better cooling efficiency and thermal comfort under summer conditions.

Petrone et al. [19] investigated air and temperature distribution inside a half cabin section of a touring bus. The flow domain is a cabin section consists of 2 consecutive seat rows with 4 passengers divided in half using the symmetry plane through the aisle. The grid structure with 360.000 nodes has been solved in steady state regime using COMSOL

Multiphysics® under the considerations of adiabatic walls by employing a Newton-Raphson method with k-ε scheme for turbulence modelling. The results indicate the best arrangement which guarantees the thermal comfort for passengers is the combination of standard ceiling system with a displacement scheme for heating air inlet.

1.3. Outline and Methodology

In this study, the temperature distribution inside a long distance bus cabin is investigated using experimental and numerical methods, similar to the analogous studies mentioned in the literature review. It can be seen that many of the previous studies use advanced CFD software for the numerical methods, similar solver types and turbulence models for these CFD software and include the validation of the numerical model with the data obtained by experimental methods. This study, however, includes the transient cooling analysis of a specific bus cabin with the consideration of the heat absorption effects of the cabin materials.

The approach in this thesis is embraced under 5 chapters.

Chapter 1 provides introductory information regarding the importance of the study, provides brief information about the cooling system of a conventional bus and outlines the state of art.

Chapter 2 explains the all the studies conducted in scope of this thesis in detail under three sections: governing equations, experimental methods and numerical methods. In the governing equations, the mathematical nature of the study, including the conservation equations, turbulence modelling, convection and conduction heat transfer and near wall equations are explained in detail. Experimental methods describes the test conducted using a full scale bus inside a climatic chamber to gather real-life information about the nature of cabin cooling. In the numerical methods section, the studies performed to obtain numerical solutions which are in agreement with the readings obtained in the experimental methods, are clarified.

Chapter 3 combines all the main findings gathered throughout the study and compares the results obtained from the experimental and numerical methods from the temperature distribution point of view on the different levels window and aisle seats.

Chapter 4 provides an overall conclusion of the study and Chapter 5 briefly states the recommendations for the possible future works.

2. THEORY, MODELLING AND EXPERIMENTAL STUDIES

In this chapter, the main activities of the whole thesis are explained in detail. The studies consist of 3 main elements, namely, the description and identification of the governing equations, the experimental methods to gather input and output parameters and the numerical methods for a comprehensive insight into the 3D flow.

2.1. Governing Equations

The governing equations in this study are Navier-Stokes equations which states that the sum of momentum changes that acts on a unit mass in a fluid equals to the sum of pressure changes and viscous forces. In a nutshell, Navier-Stokes equations are the dynamical expression of the force balance in a specified region within the fluid.

Navier–Stokes equations are derived from the conservation of mass (2.1), momentum (2.2) and energy (2.3) equations which can be written as:

$$\frac{\partial \rho}{\partial t} + \frac{\partial \rho u_i}{\partial x_i} = 0 \tag{2.1}$$

$$\frac{\partial \rho u_i}{\partial t} + \frac{\partial \rho u_i u_j}{\partial x_j} = -\frac{\partial P}{\partial x_i} + \frac{\partial}{\partial x_j}\left[\mu\left(\frac{\partial u_i}{\partial x_j} + \frac{\partial u_j}{\partial x_i}\right)\right] \tag{2.2}$$

$$\frac{\partial \rho T}{\partial t} + \frac{\partial \rho T u_j}{\partial x_j} = \frac{\partial}{c_p \partial x_j}\left(k\frac{\partial T}{\partial x_j}\right) \tag{2.3}$$

where ρ is the density, μ the kinematic viscosity, u the velocity, P the pressure, T the temperature, t the time, x_i the x, y, z position tensor, c_p the specific heat capacity and k the thermal conductivity.

Since density stays constant in the incompressible flows, the conservation equations can be rearranged as follows:

$$\frac{\partial u_i}{\partial x_i} = 0 \tag{2.4}$$

$$\rho \frac{\partial u_i}{\partial t} + \rho \frac{\partial u_i u_j}{\partial x_j} = -\frac{\partial P}{\partial x_i} + \frac{\partial}{\partial x_j}\left[\mu\left(\frac{\partial u_i}{\partial x_j} - \frac{\partial u_j}{\partial x_i}\right)\right] \tag{2.5}$$

$$\rho \frac{\partial T}{\partial t} + \rho \frac{\partial T u_j}{\partial x_j} = \frac{\partial}{c_p \partial x_j}\left(k \frac{\partial T}{\partial x_j}\right) \tag{2.6}$$

2.1.1. Turbulence Modelling

All flows encountered in engineering practice above a certain Reynolds number are observed to become turbulent. Turbulence can be stated as a chaotic and random state of motion develops in which the velocity and pressure change continuously with time within the flow [20].

Solving the governing equations for a turbulent flow is extremely difficult without several considerations and simplifications. One of these simplifications are Reynolds-Decomposition method which divides flow variables of Navier-Stokes equations into mean and fluctuating components. In this case the velocity and pressure can be expressed as

$$u_i = U_i + u_i' \tag{2.7}$$

$$p = P + p' \tag{2.8}$$

Where U and P are the mean and u_i' and p' are the fluctuating components of the velocity and pressure, respectively.

By placing these equations into the governing equations, Reynolds-averaged Navier-Stokes (RANS) equations would be derived:

$$\frac{\partial U_i}{\partial x_i} = 0 \tag{2.9}$$

$$\rho \frac{\partial U_i}{\partial t} + \rho U_j \frac{\partial U_i}{\partial x_j} = -\frac{\partial P}{\partial x_i} + \frac{\partial}{\partial x_j}\left[\mu\left(\frac{\partial U_i}{\partial x_j} - \overline{u_i' u_j'}\right)\right] \tag{2.10}$$

$$\rho\frac{\partial T}{\partial t}+\rho\frac{\partial Tu_i}{\partial x_j}=\frac{\partial}{C_p\partial x_j}\left[k\left(\frac{\partial T}{\partial x_j}\right)\right] \tag{2.11}$$

where $\overline{u_i'u_j'}$ is the Reynolds stress tensor which states the stress caused by the velocity fluctuation inside the turbulent flow.

In this study, the realizable k-ε turbulence model is used, which has been extensively validated for a wide range of flows and its performance found to be substantially better than that of the standard k-ε model [21]. Besides the consistency of this model in many flow and heat transfer problems, it is also serves as an ideal model in terms of calculation time.

For the continuous and incompressible flows, transport equations for turbulent kinetic energy k (2.12) and dissipation ε (2.13) is defined as follows:

$$\frac{\partial}{\partial t}(\rho k)+\frac{\partial}{\partial x_j}(\rho k u_j)=\frac{\partial}{\partial x_j}\left[\left(\mu+\frac{\mu_t}{\sigma_k}\right)\frac{\partial k}{\partial x_j}\right]+G_k+G_b-\rho\varepsilon-Y_M+S_k \tag{2.12}$$

$$\frac{\partial}{\partial t}\rho\varepsilon+\frac{\partial}{\partial x_j}(\rho\varepsilon u_j)=\frac{\partial}{\partial x_i}\left[\left(\mu+\frac{\mu_t}{\sigma_\varepsilon}\right)\frac{\partial \varepsilon}{\partial x_j}\right]+\rho C_1 S_\varepsilon-\rho C_2\frac{\varepsilon^2}{k+\sqrt{v\varepsilon}}+ C_{1\varepsilon}\frac{\varepsilon}{k}C_{3\varepsilon}G_b+S_\varepsilon \tag{2.13}$$

$$C_1=max\left(0{,}43\frac{\eta}{\eta+5}\right) \tag{2.14}$$

$$\eta=S\frac{k}{\varepsilon} \tag{2.15}$$

$$S=\sqrt{2S_{ij}S_{ij}} \tag{2.16}$$

where G_k is the generation of turbulence kinetic energy due to the mean velocity gradients, G_b the turbulent kinetic energy generated due to buoyancy, Y_M contribution of the fluctuating dilatation in compressible turbulence to the overall dissipation rate. Y_M is only important in the high Mach numbers. C_2 and $C_{1\varepsilon}$ are constants and σ_k and σ_ε are the turbulent Prandtl numbers for k and ε respectively.

2.1.2. Natural Convection Using the Boussinesq Approximation

Buoyancy is defined as the streams which occurs due to the local density changes within the fluid and gains momentum due to a number of effects like gravity or centrifugal forces. These streams which originate only from the temperature gradients are called natural convection and forms a situation which the heated and fluid displaces in the opposite direction of the gravity.

In consideration of temperature differences in the flow domain, a density variation, therefore a result of the buoyant forces must be taken into account. The general expression of this flow attitude can be written in the form as:

$$\frac{D\rho}{Dt} + \nabla\,(\rho u) = 0 \tag{2.17}$$

where ρ is the density and u is the local velocity. By reason of the density variations are negligible based the Boussinesq approximation which converts the equation as:

$$\nabla\,.\,u = 0 \tag{2.18}$$

$$\frac{Du}{Dt} = -\frac{1}{\rho_o}\nabla\,Pu - \frac{1}{\rho_0}F + \nu\nabla^2 u \tag{2.18b}$$

where ρ_o is the constant density of the fluid, P the pressure, ν the kinematic viscosity and F is the body force. The terms on the right side of the equation are the pressure force in the fluid flow, the buoyant force represented by $F = (\rho - \rho_0)g$ which is generated by the density variation and the viscous force respectively.

Since the density variation occurs as a result of temperature difference in the fluid, temperature is included in the equation by means of a material property called the thermal expansion coefficient, β. Fluent solver takes density as a constant value in the conservation equations except the buoyancy term in the momentum equation:

$$F = (\rho - \rho_0)g \approx -\rho_0\beta(T - T_0)g \tag{2.19}$$

Substituting (2.19) into the equation (2.18b), the momentum equation becomes:

$$\frac{Du}{Dt} = -\frac{1}{\rho_0}\nabla p - g\beta(T - T_0) + \nu\nabla^2 u \tag{2.20}$$

2.1.3. Convection Heat Transfer on Window and the Walls

The convective heat transfer coefficient measures the amount of convective heat flux which develops between the solid walls and the fluid as a result of the temperature difference and bulk motion. This phenomenon can be defined with the Newton's law of cooling:

$$q_{conv} = h(T_s - T_\infty) \tag{2.21}$$

Where q is the convective heat flux, h the heat transfer coefficient, T_s the temperature on the solid wall and T_∞ the temperature of the fluid in contact with the wall.

2.1.4. Conduction Heat Transfer on the Walls

Conduction heat transfer is occurred inside the solid walls and the temperature gradient is directed from the warm side (outer air side) to the colder side of (cabin side) of the walls. Conduction heat transfer is governed mathematically by Fourier's law (2.22) where q is the heat flux, dT/dx the heat gradient and k the thermal conductivity which might be a function of temperature or a matrix for anisotropic materials, but is a scalar value for isotropic materials.

$$q_x'' = -k\frac{dT}{dx} \tag{2.22}$$

2.1.5. Near Wall Region

In wall bounded flow simulations, like cabin flows, near wall treatment strategy is a key issue since solid walls are one of the main sources of turbulence. To precisely capture the flow near the walls, the mesh structure near the wall boundaries are of extreme importance. This is where the y+ phenomena should be introduced.

y^+ is a dimensionless wall distance described at the first layer of grid near to a wall which describes how fine or coarse the mesh near the wall for wall bounded flows. The turbulent flow can be expressed in three different sub-regions based on y-plus value: The wall shear is dominated by 1) viscous stress in viscous sublayer, 2) by turbulent shear in log-law and 3) by both viscous and turbulent shear in buffer region (Table 2). For CFD analysis, the most crucial one is the viscous sublayer which stands slightly further away from the wall where the velocity changes rapidly:

$$y^+ \equiv \frac{u_\tau y}{\nu} \tag{2.23}$$

where y is the distance from the wall, ν the kinematic viscosity and u_τ the friction velocity defined as

$$u_\tau \equiv \sqrt{\frac{\tau_w}{\rho}} \tag{2.24}$$

where τ_w is the shear wall stress and ρ the density.

Table 2. Subsections of the near wall region

y^+ value	Region	Feature
$y^+ < 5$	Viscous sublayer region	Viscous stress dominates
$5 < y^+ < 30$	Buffer region	Both viscous and turbulent shear dominate
$30 < y^+ < 300$	Fully turbulent portion of the log-law region	Turbulent shear predominates

A turbulent boundary layer consists of distinct regions shown in the. In practice, the simulation presents the best result if $y^+ < 5$ [22].

2.2. Experimental Methods

An experiment using a full scale bus is conducted in order to obtain realistic input parameters to be used in the CFD analysis of a cabin section. The main objective of the experiment is to determine time-dependent values of the input air temperatures supplied to the cabin from the service units and from the roof inlets in order to be used as input parameters in the CFD analysis.

Another objective of the test is to determine the time-dependent temperatures in the head, knee and foot levels of the seats in order to compare these values with the CFD analysis results and to validate the geometry and the parameters used in the CFD model.

2.2.1. Experiment Conditions

Before the experiment, 3 main factors have been determined: 1) type of the test specimen, 2) operating parameters to be used in the test and 3) test facility.

Since the effects of the conceptual zonal air-conditioning can be best observed in long journeys, the type of the vehicle is selected as a long distance bus. Considering the market segmentation of any future climatic system improvement based on this study, the vehicle is selected from the premium segment. To eliminate the effects of wear, tear and unexpected aftermarket modifications on the overall system and to reach more accurate results, a used vehicle from the vehicle park is avoided. As a result, Neoplan Tourliner (P21) coming right out of the from the production line is selected as the test vehicle.

Considering the validation objective of the experiment, the operating conditions of the experiment are selected as realistic as possible to be used in the CFD analysis. The outer temperature is selected as 45°C which is commonly used in the air conditioning performance tests of the MAN Truck & Bus AG and the target cabin temperature for the A/C unit is selected as 24°C which is commonly considered as the comfort temperature for passengers. A/C fan speed is set to a constant value to avoid the time-dependent fluctuations in the inlet air velocities and eliminating a variable parameter to shorten the CFD calculation times.

Since the objective of the experiment is not to perform a cooling performance test but only to obtain the change of air inlet temperatures over time, fan speed setting is selected as 60%.

The test facility is selected as the Environmental Test Center of OTOKAR in Sakarya, TR which is dimensionally suitable to fully enclose a coach, satisfying the required temperature interval and located within a reasonable range to the plant.

2.2.2. Measurement Layout and Instrumentation

In order to prepare a measurement layout; a good understanding of the effective parameters to be measured, the location of these measurements and the capabilities and availability of the measurement tools are required.

The vehicle consists of 13 seat rows which includes 4 seats at each row of which are separated by a hallway along the vehicle. Conditioned air is provided to the cabin via 1) the adjustable ducts on the service units located above the seats and 2) fixed ducts placed along the side of the air vent opening to the hallway. The cabin air is exhausted via the openings located on the window side of the air vent. For every 2 seats on a seat row on each side of the bus there are 2 inlets on the service unit and 2 inlets on the roof and one outlet on the window side of the air vent.

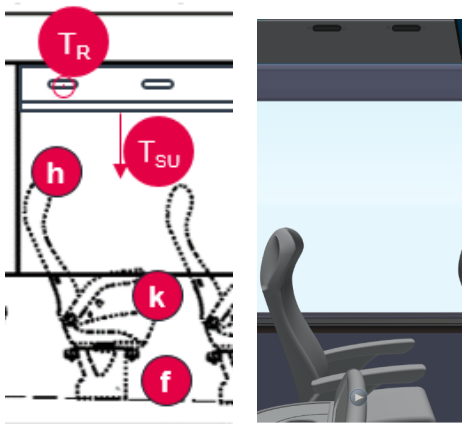

Figure 3. Schematic view of the cabin section

For the time dependent temperature measurements, a total of 24 K-type SAB-Bröckskes thermocouples are connected to Panasonic CF-29 Toughbook via 2 QAETEC

QIC Thermo 16 dataloggers. For the measurement of instantaneous inlet air velocities, anemometers with Testo T435-4 multimeter and Testo T400 hot-wire probes are used (Figure 4).

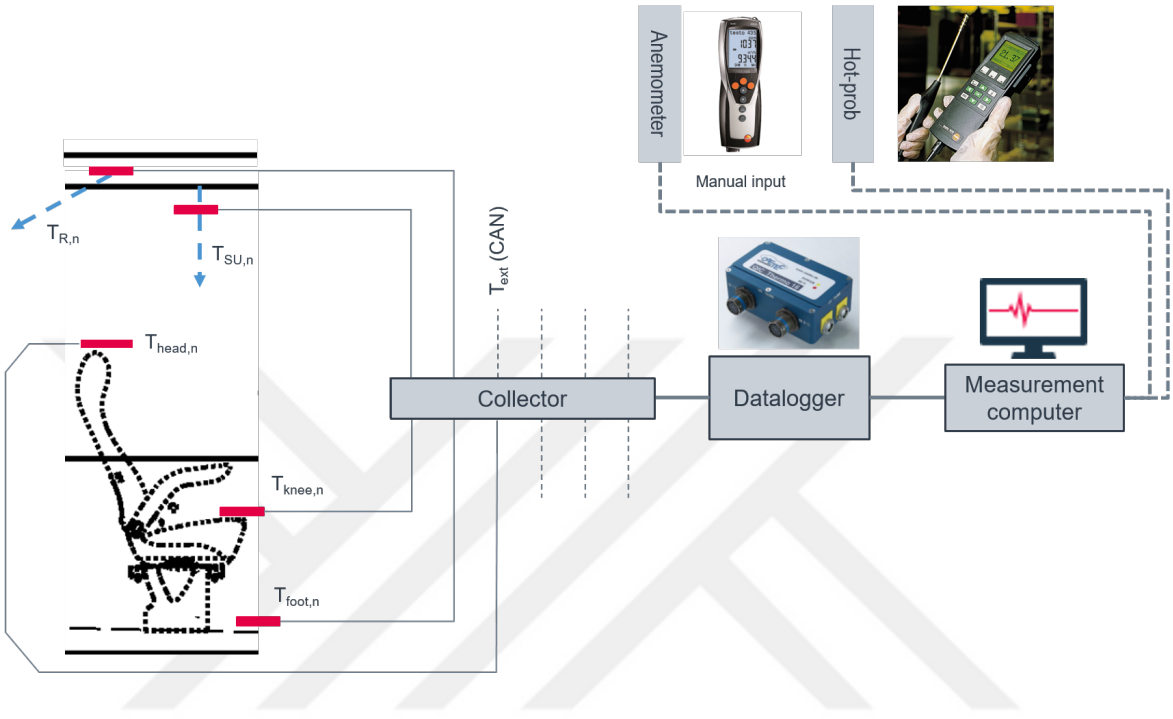

Figure 4. Instrumentation layout

Figure 5. Thermocouple positions on the seats

General application embraced in passenger thermal measurement for buses is to collect data in 3 different levels of the seat for each passenger: T_{head}, T_{knee} and T_{foot}. Since the datalogger used in this experiment has 32 available channels in maximum, the number of time-dependent measurement points using the thermocouples is limited. Therefore it is decided to take measurements from both the window and aisle seats in the 2nd, 8th and 12th seat rows on the left hand side of the coach – since the air vent continuously lies along the bus unlike the air vent on the right hand side which is segmented into 2 due to the head clearance required in the middle doorsteps (Figure 6).

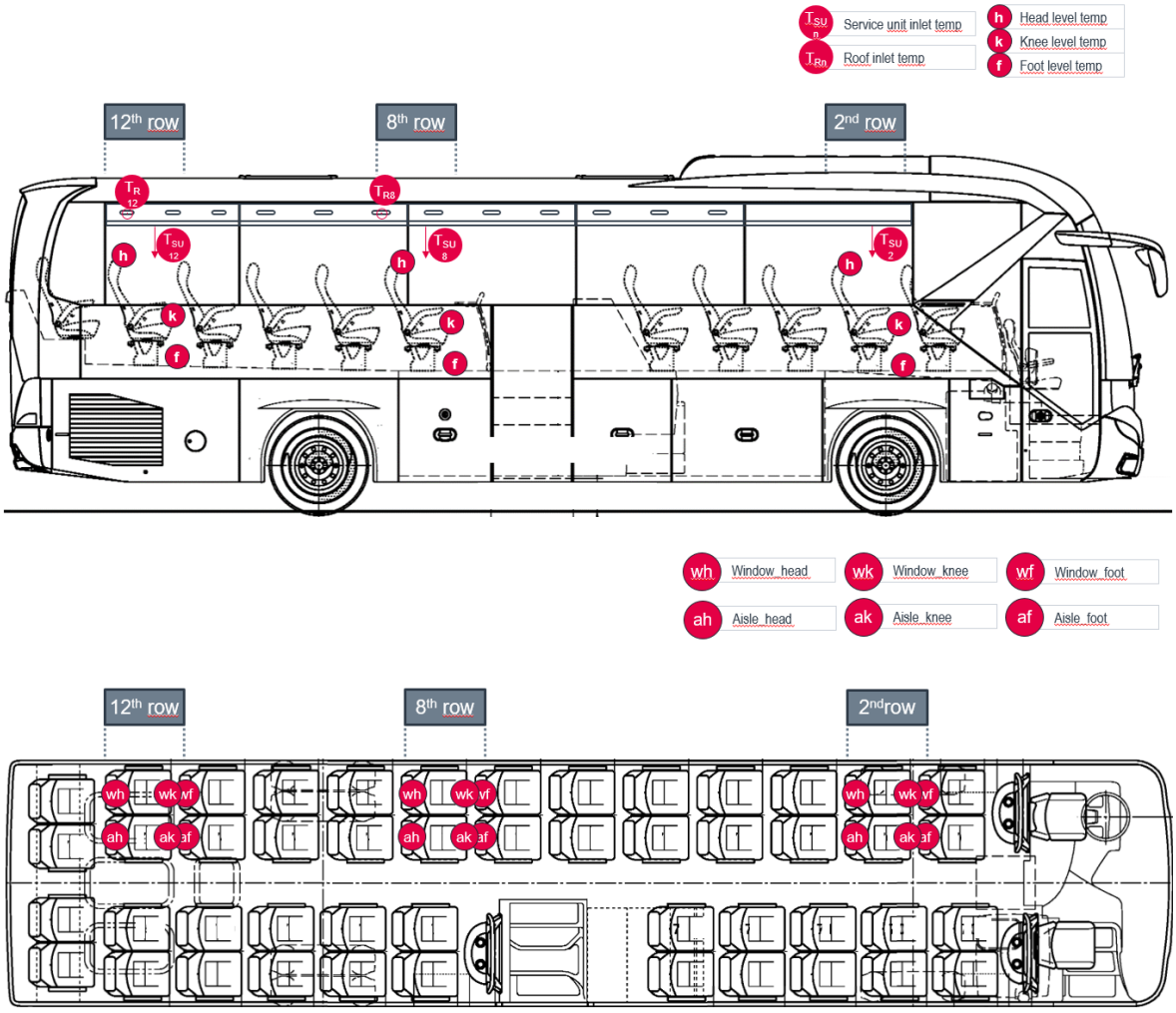

Figure 6. Layout of the measurement points

2.2.3. The Experiment

The instrumented vehicle is placed inside the climatic chamber and the exhaust discharge is mounted. In order to provide a faster thermal equilibrium inside the cabin, passenger doors, side flaps and roof hatches are opened and portable air fans are located in front of the doors. Since the actual blowing angle from the adjustable service units cannot be precisely measured during the experiment, each air duct on these units are adjusted normal to the opening surface. The target temperature of the climatic chamber is set to 45°C and the vehicle is left inside the chamber to reach thermal equilibrium for 3 hours.

When most of the temperature readings from the different points of the vehicle reached 45°C, the engine is started and data recording began. A/C unit turned on and the desired temperature setting inside the cabin is adjusted to 24°C. The engine is revved up to 1500 rpm using an adjustable footstep.

The recording last for 90 minutes and during the experiment, air velocities from the air inlets of different seat rows have been manually measured time to time.

2.2.4. Experiment Results

Since the fan speed is manually set to a constant value (60%) in the favour of keeping the inlet velocities constant, the A/C unit cannot succeed to bring the cabin temperature to the desired target temperature (24°C) within the test duration. It is also observed that the climatic chamber could not keep the external temperature constant at 45°C and shows a slight inclination to 50°C over time. However, a detailed ‘temperature vs. time’ values of a cooling operation for a coach have been obtained to be further used as input and validation parameters for any CFD cooling analysis of a long distance coach, as planned. The graphics clearly state that the temperature of the air supplied by the A/C unit is not constant and decreasing over time to bring the average temperature in the cabin to the desired target temperature set by the driver (Figure 7, Figure 8).

It can also be stated that the seat temperatures follows the air inlet temperatures with a constant temperature difference of ~10°C (Figure 9).

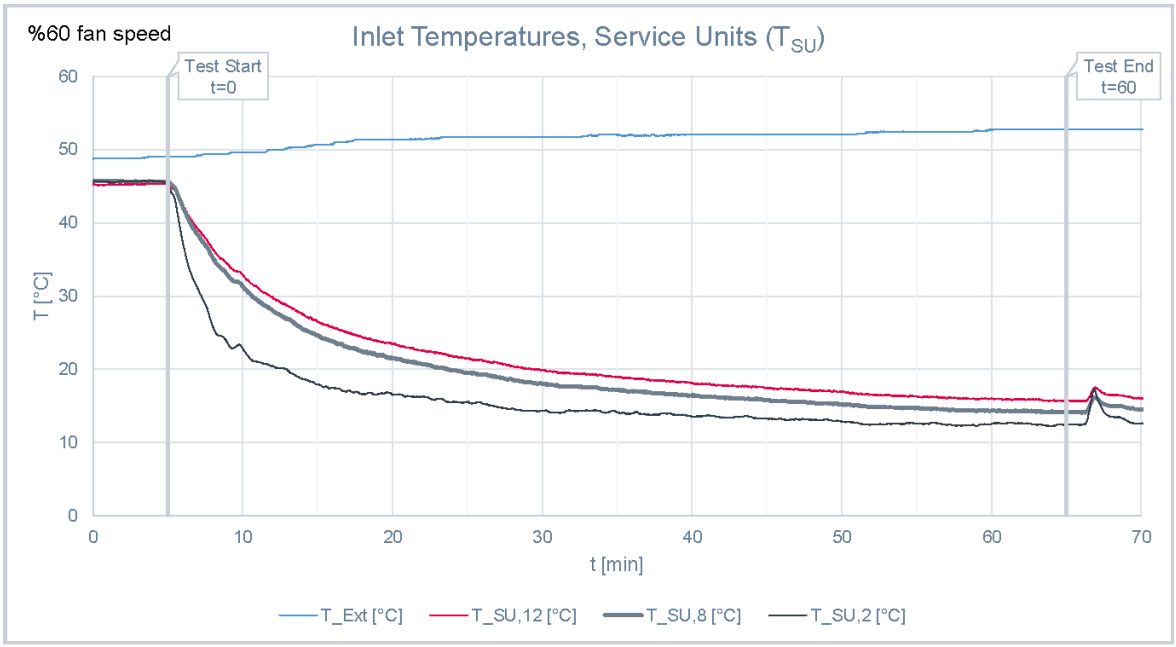

Figure 7. Inlet temperatures of the service units over time

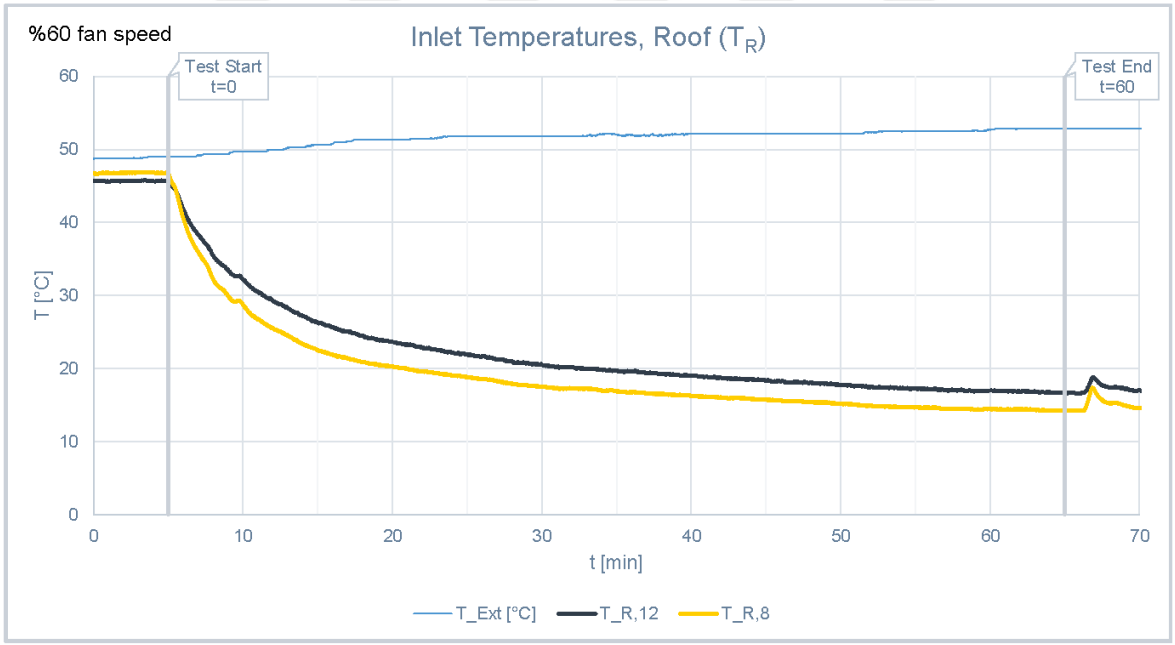

Figure 8. Inlet temperatures of roof openings over time

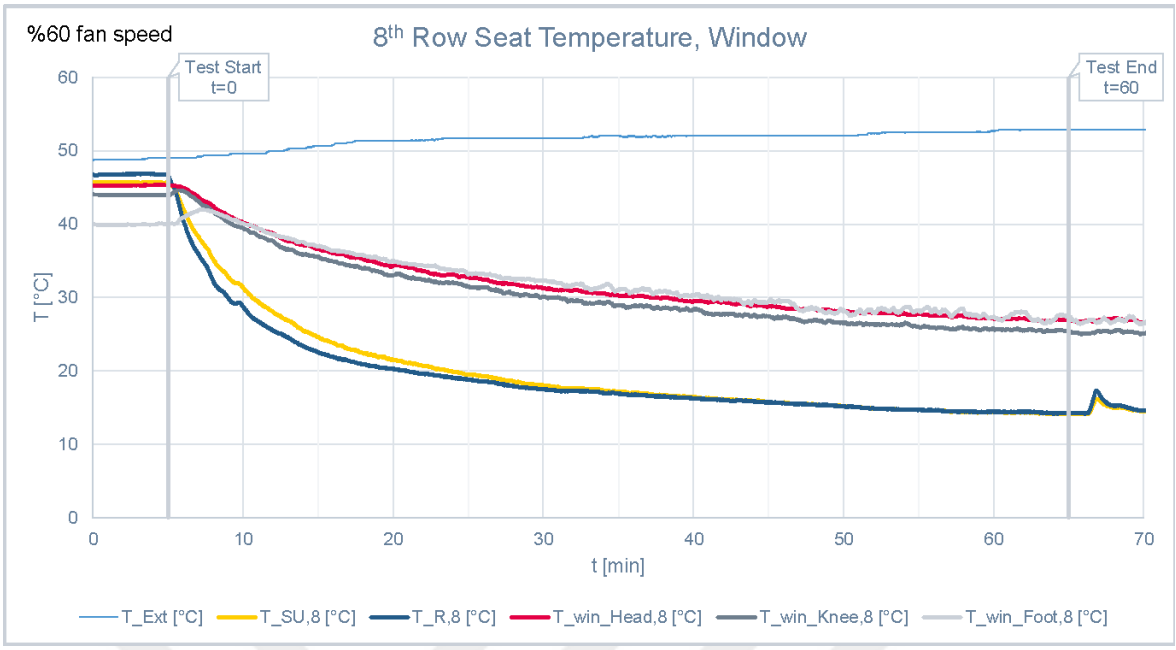

Figure 9. Inlet and seat temperatures for the window seat at the 8th row

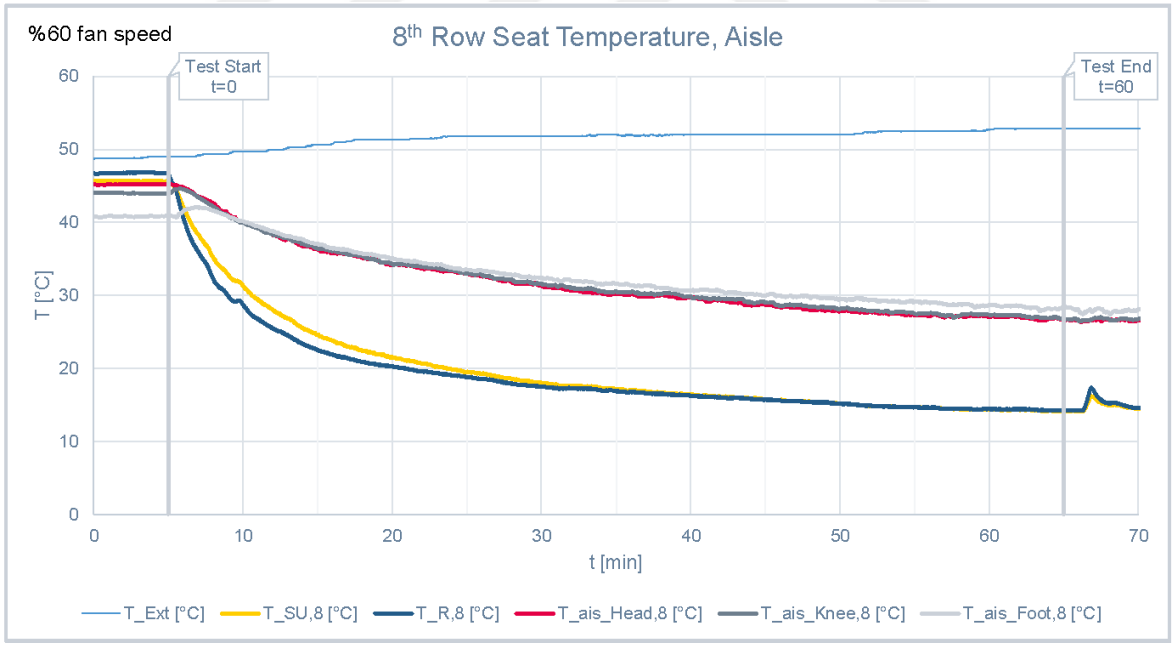

Figure 10. Inlet and seat temperatures for the aisle seat at the 8th row

In the measurement of inlet air velocities, an anemometer and a hot-wire probe is used. Several measurements using the anemometer during the experiment proves that the air

inlet velocities remain constant over time, as expected. Since the service unit inlets have a perforated structure due to the built-in fins, air velocity varies across the different points on the inlet. For a better representation of the velocity profile at the inlet, air velocities from multiple points on the service unit are measured using the hot-wire probe.

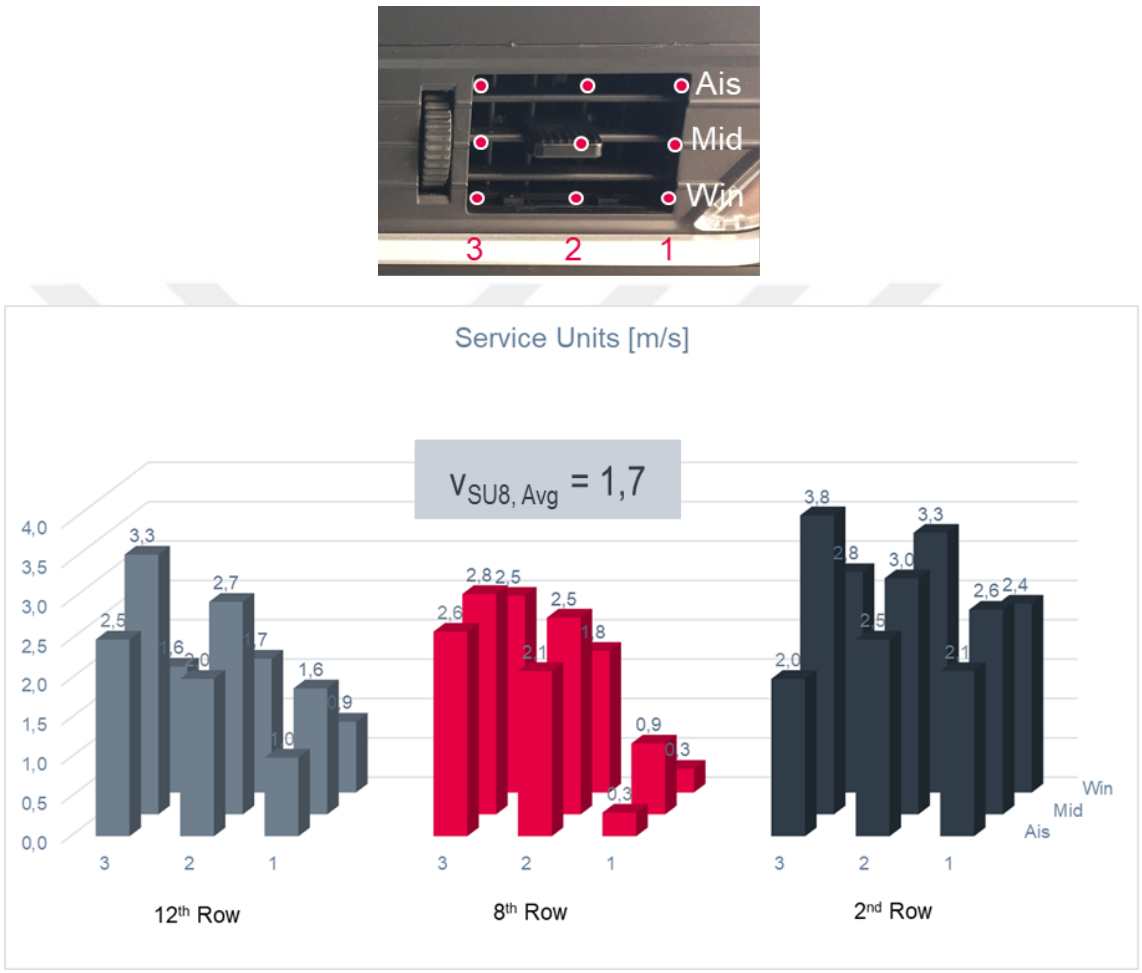

Figure 11. Measurement points (above) and inlet velocities (below) on the service units

2.3. Numerical Methods

The objective of the numerical methods is to obtain a validated CFD model which reflects the thermal behaviour of an actual bus cabin responsive to inlet parameters and boundary conditions that eliminates or minimizes the necessity to further physical experiments to an extent.

The workflow to be followed in the numerical methods starts with the problem identification and preparation of the cabin geometry, followed by grid generation and ends with validating the model.

2.3.1. Problem Identification

In the most simplest form, the cabin model of the bus consists of a watertight enclosure having multiple layers of materials, multiple passenger seats, multiple inlets and outlets and filled with air inside the enclosure. The modelling goals are defined as to obtain the temperature readings on the 3 different levels of the window and aisle seats –similar to those obtained in the experimental methods.

For the favour of reasonable calculation times, the problem is simplified with a number of assumptions: Instead of modelling the whole cabin, a section of the cabin consisting only one seat row with a periodic boundary condition in the front and rear section faces is assumed to reflect the general thermal behaviour for the most of the cabin volume. Since the right and left side of the cabin is very similar throughout the aisle, the cabin section is considered symmetrical from the imaginary plane on the aisle separating the cabin into right and left.

At the beginning of the flow domain and physical model identification, the flow domain was selected as the air volume inside the cabin with the seats subtracted and the physical models were identified as 1) the natural convection inside the flow domain, 2) convection heat transfer on the windows and 3) adiabatic assumption for the most of the cabin walls, similarly to the analogous studies [9, 19, 23]. However, the first trials clearly prove that 1) the heat absorbed by the seats and 2) instead of adiabatic boundary condition for the walls, conduction with multiple layers should be taken into consideration. It is also assumed that the exterior temperature is constant and the analysis geometry is watertight.

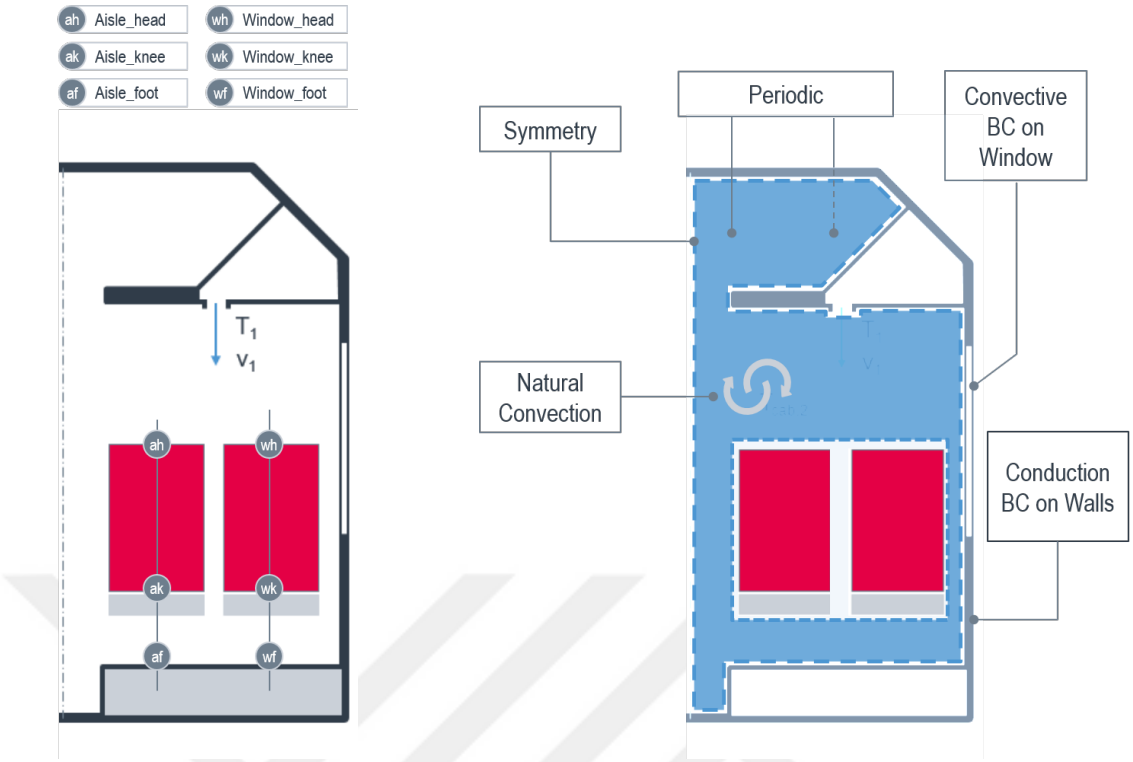

(a) (b)

Figure 12. An illustration of the modelling goals (a) and the boundary conditions (b)

2.3.2. Creating the Analysis Geometry

The test vehicle, Neoplan Tourliner with the chassis number P212039, is a high floor long distance bus having the dimensions of 12 m in length, 2,5 m in width and 3,8 m in height. The vehicle has 13 seat rows and a total of 48 passenger seats. The full cabin assembly data is obtained from the CATIA servers of the MAN Truck & Bus, however due to the intensity of flow-irrelevant components, the data was very large in file size (>2,8 GB) and redundantly complex to be handled by CFD analysis software (Figure 13).

The strategy followed in the creation of the analysis geometry starts with identification and classification of the main and sub components followed by separate simplification of the components and ends with the classification of the components according to their effects on the flow domain. Apart from all the fasteners, connectors and constructional components that are not the focus of the flow domain, the main components and their sub-components are listed and evaluated as in the Table 3. Considering the

convergence behaviour and the computational time required, the components with high geometrical complexity and low effect on the analysis are decided to be excluded from the analysis geometry (Table 3).

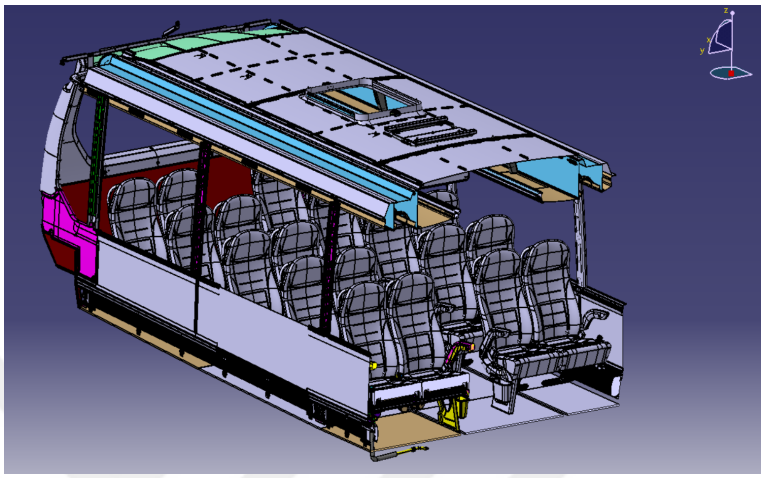

Figure 13. Section view of the full cabin geometry of the bus

Table 3. Classification of the components for simplifying the analysis geometry

	Effect on flow-domain	Geometrical complexity	Decision
1. **Cabin**			
a. Floor	High	Low	Include in the analysis
b. Side walls	High	Low	Include in the analysis
c. Side glass	High	Low	Include in the analysis
d. Roof	High	Low	Include in the analysis
e. Side wall coverings	Med	Med	-
f. Pillar coverings	Med	Med	-
g. Convector heaters	Med	Med	-
2. Seats			
a. Backrest	High	Med	Include in the analysis
b. Bottomrest	High	Med	Include in the analysis
c. Armrest	Low	High	-
d. Footrest	Low	High	-
e. Mounting racks	Low	High	-
f. Handles	Low	High	-
g. Service table	Low	High	-
h. Seat net	Low	High	-
3. Air vent			
a. Service unit ducts	High	Med	Include in the analysis
b. Corridor ducts	High	Low	Include in the analysis
c. Outlet ducts	High	Low	Include in the analysis

3D models of the cabin, seats and air vent are separately imported and simplified and re-assembled using ANSYS SpaceClaim®. The sub-components having a negligible effect on the flow characteristics have been removed, the sharp edges and ‘spikes’ on the components are rounded and the number of faces are decreased to simplify the meshing process. Seat assembly, for instance, is cleared from the accessories like the armrests, back handles, seatbelt buckle and leaning mechanism which are not directly relevant with the flow domain and the data file size has been dramatically reduced from 92 MB to 1 MB (Figure 14). Cabin enclosure and air vents have also been similarly simplified and re-assembled (Figure 15). After these procedures, the flow domain is extracted from the cabin geometry as one solid body (Figure 16).

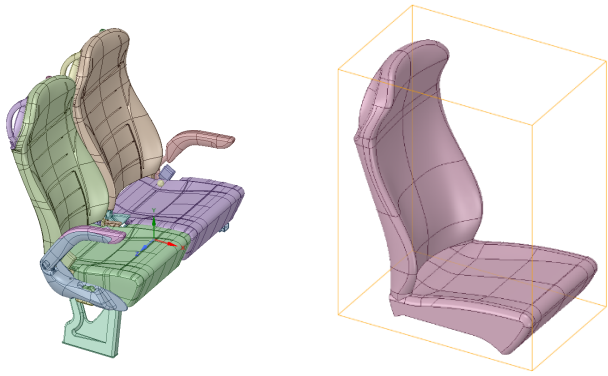

Figure 14. Seat assembly before (left) and after the simplifying process (right)

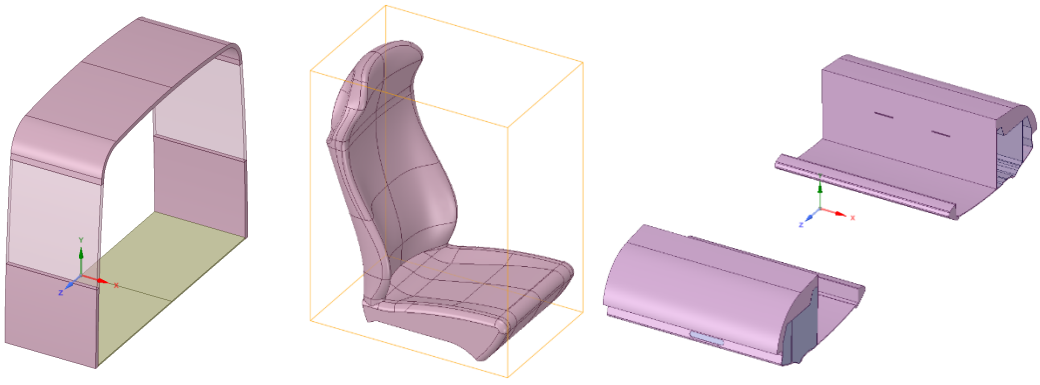

Figure 15. The simplified cabin (left), seat (middle) and the air vents (right)

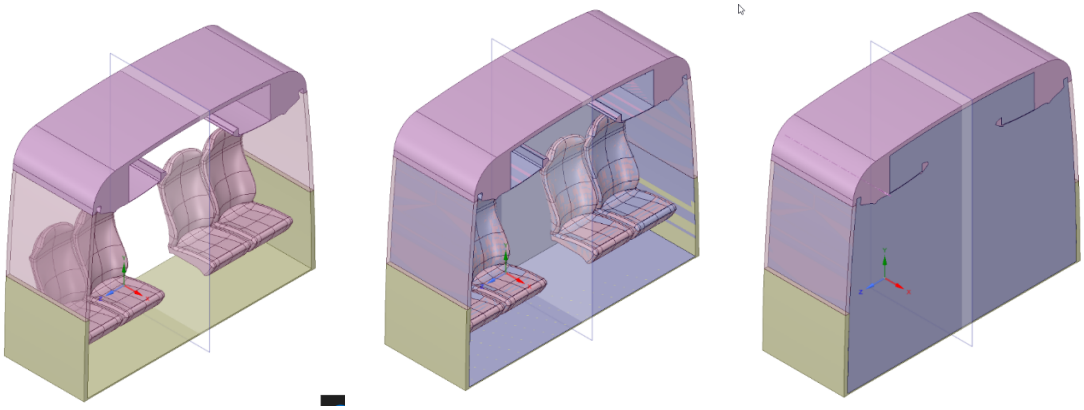

Figure 16. Volume extract process of the flow domain

2.3.3. Grid Generation

ANSYS Fluent solvers are based on the finite volume method, which the fluid domain is discretized into a finite set of volumes which is called “grid” or “mesh” structure. In this study, the volume mesh is created using Fluent Meshing® which allows ‘shrink wrapping’ the geometry for a higher mesh quality and the creation of polyhedral meshes which reduces the total number of cells, hence, the amount of calculation time.

The strategy on meshing starts with identifying sizing to the inlets and outlets followed by creating ‘inflations’ near the wall faces to capture the boundary layer, and finally ‘wrapping’ the faces for achieving higher orthogonal quality and lower skewness values and creating polyhedral elements to the wrapped surface.

The geometry has 2 roof inlets, 2 service unit inlets and one outlet. Since the flow characteristics near these regions can have serious effects on the bulk region, where most of the temperature readings will take place, the grid around the inlets and outlets are of intensive importance. Therefore, a total of 4 sizing controls have been applied to the imported geometry which are listed in the Table 4 below. The effect of curvature and proximity sizing controls applied to the inlets can be observed from the Figure 17 and Figure 18.

Table 4. Sizing controls of the base mesh

	Sizing Control	Scope to	Local min-max	Growth rate / angle	Cells per gap
1	Curvature to all volume	Object face & edges	1,0 – 25 mm	1,2 / 30°	-
2	Curvature to inlet & outlet edges	Edge zones	1,0 - 25 mm	1,2 / 30°	-
3	Proximity to inlet & outlet edges	Edge zones	0,5 – 25 mm	1,2 / 30°	6
4	Proximity to inlet & outlet faces	Face zones	0,5 – 25 mm	1,2 / 30°	6

In order to capture the flow regime near the walls, a special type of grid (boundary layer mesh) should have been formed. In the base mesh, a scoped boundary layer mesh having 5 layers having a 1st aspect ratio of 10 and a growth rate of 1,2 has been applied to all of the faces of the geometry except the inlets, outlets, periodic and symmetry faces. The 'inflation' near the wall regions can be observed from Figure 18.

Wrapping the internal surface of the object has drastically decreased the number of free faces, multi faces and skewed faces to zero and provides a maximum skewness of 0,64 in the surface mesh. Creating a volume mesh based on this surface mesh concluded with around 1 million cells having a maximum skewness of 0,79 and minimum orthogonal quality of 0,30 which is considered to be adequate to resolve the flow characteristic of the cabin.

In this study, 2 mesh models of the cabin is created: 1) air volume mesh with the seats extracted, 2) air volume mesh with the seats meshed. The two different mesh models with the 'hollow' seat-zones and the 'solid' seat zones filled up with polyhedral elements can be seen in the Figure 19.

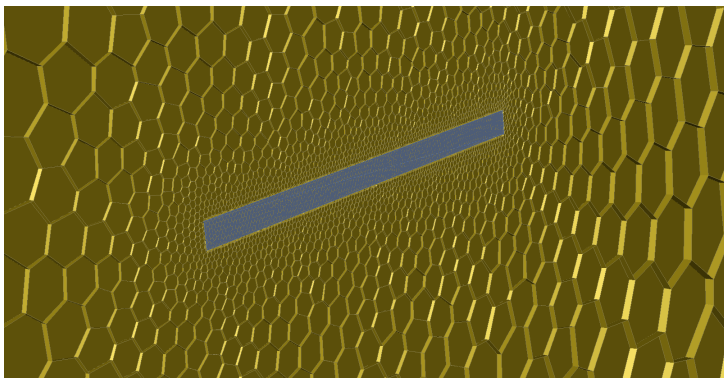

Figure 17. Mesh structure in the roof inlet

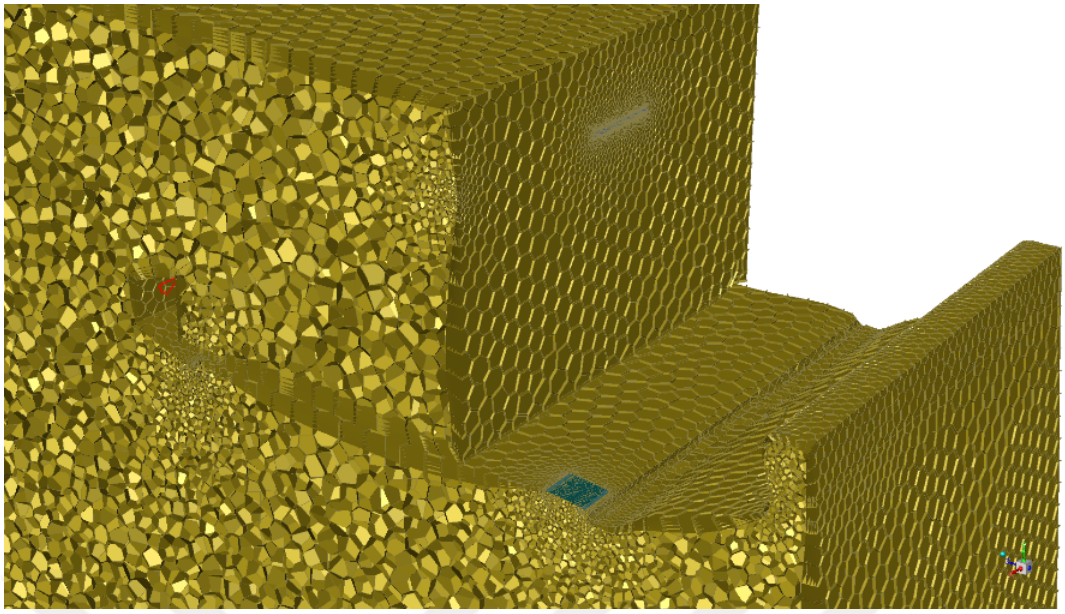

Figure 18. Sectional view of the cabin mesh

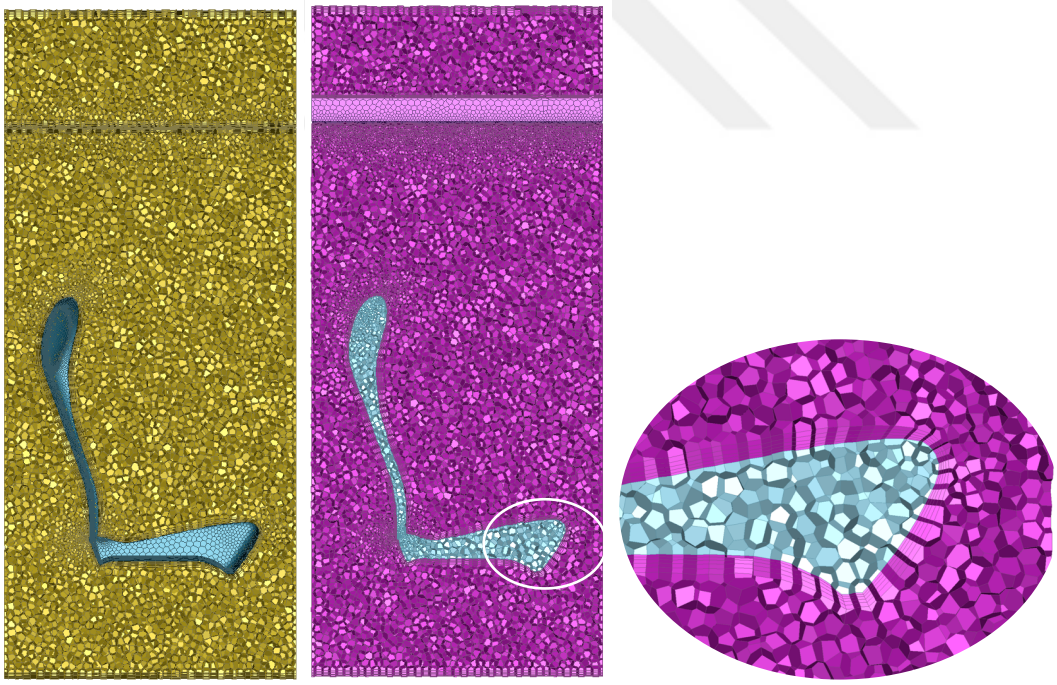

(a) (b)

Figure 19. Mesh 3.0 with hollow seats (a) and Mesh 3.1 with the seats meshed (b)

2.3.4. Validating the Model

The numerical solver selected for this study, ANSYS Fluent, is a commercial CFD software which solves aforementioned continuity, momentum and energy equations numerically by using the finite volume method for predicting the fluid flow, heat and mass transfer and related phenomena. In the numerical solutions, the fluid domain is discretized into a finite set of control volumes, partial differential equations are discretized into a system of algebraic equations and these equations are solved numerically to render and to provide a visual expression of the solution field.

For ANSYS Fluent to perform in a way that is similar to the experimental methods, a consistent solver setup must be created. In the creation of the solver setup, the solver type and time, the physical models, the properties of the materials, the boundary conditions and the positions of the monitoring points and monitor types must be identified and correctly introduced in the model. Afterwards, a grid independent solution is tried to be achieved.

2.3.4.1. Solver Setup

ANSYS Fluent has 2 types of solver: pressure-based and density based. Considering the density based solver is generally applicable for special cases like capturing shock waves in very high Mach numbers, pressure based solver is selected in this study. Due to the time dependent nature of the experimental conditions which is tried to be validated, time setting is selected as “Transient”.

For the pressure based solver, a pressure-velocity coupling is required which the Fluent Solver has a number of alternative methods like SIMPLE, SIMPLEC, PISO and Coupled. In this study, SIMPLE is selected considering its proven convergence behaviour in the analogous studies [10, 14, 17].

2.3.4.2. Physical Models

For the reflection of the physical models identified in the problem identification section, the energy equations are turned on and for modelling the turbulent flow inside the air volume, “realizable k-ε turbulence model” with “enhanced wall treatment” are selected

[10, 11, 12, 17, 19]. In this study, the enhanced version of the k-ε model, the "realizable k-ε" is used since it has an alternative formulation for the calculation of the turbulent viscosity which satisfies certain mathematical constraints on the Reynolds stresses, consistent with the physics of the turbulent flows [21].

2.3.4.3. Material Properties

In the initial consideration of cabin air as the only material in the flow domain, air with "boussinesq approximation" is introduced to the solver setup. However, under the observation of the unsatisfactory alignment of the experimental and the numerical results, the introduction of solid materials to simulate the absorbed energy of the seats and heat transfer from the wall layers becomes a necessity for the proper representation of the experimental conditions in the numerical model (Table 5).

Table 5. Material properties used in the model

	Name	Material	Thickness (mm)	Density ρ (kg/m³)	Specific Heat c_p (J/kgK)	Thermal Conductivity k (W/mK)
1	Air	Air	-	1,18 [24]	1006,43 [24]	0,0242 [24]
2	Seat cushion	Polyurethane	-	70 [25]	2996 [26]	0,050 [25]
3	Interior trim	ABS	3	850 [25]	1440,76 [25]	0,188 [27]
4	Insulation	Melamine	40	9,5 [28]	2300 [25]	0,035 [28]
5	Exterior wall	Steel	1	8030 [24]	502,48 [24]	16,27 [24]
6	Plywood	Wood	15	700 [24]	1215 [29]	0,120 [29]
7	Resilient floor	PVC	2	1300 [30]	880 [31]	0,190 [31]
8	Lamilux	FRPC	2	1400 [32]	1130 [33]	0,210 [32]
9	Tempered Glass	Glass	10	2500 [34]	800 [34]	0,800 [34]

2.3.4.4. Boundary Conditions

As mentioned previously in the problem identification section, symmetry, periodic, convective, conductive and temperature boundary conditions (BCs) has been applied in the CFD model (Figure 20).

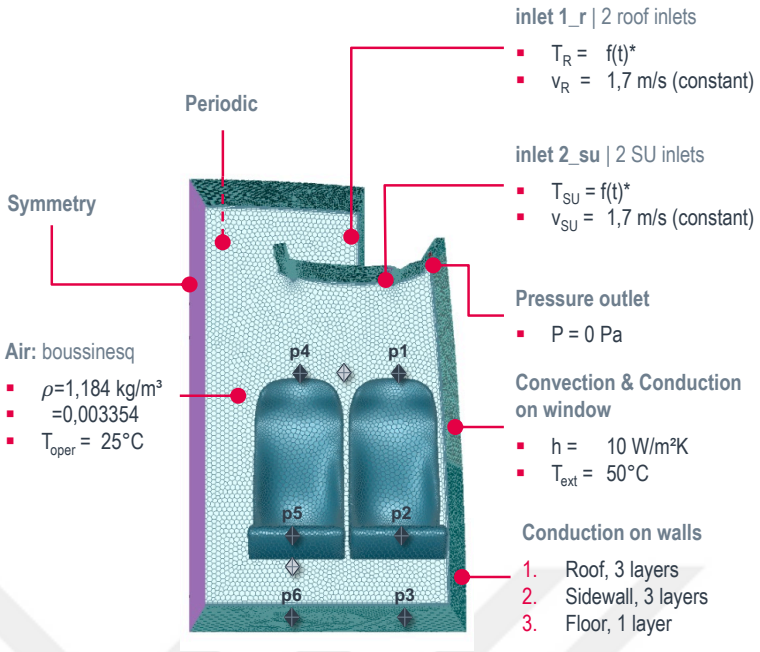

Figure 20. Boundary conditions applied on the model

In order to decrease the amount of cells to save precious amount of calculation time, only a half section of the cabin which is assumed periodic on the front and rear faces and symmetrical in the aisle surface is modelled. Therefore, periodic BC and symmetry BC are identified in the front/rear and aisle faces respectively.

Since the cabin to be cooled is placed inside a climatic chamber which has a constant exterior temperature of 50°C, the convective BC is applied to the cabin walls, namely roof, window, sidewall and the floor, to simulate the convective heat transfer between the hot external air and the cabin surroundings. Considering the vehicle is steady and the external air inside the climatic chamber does not move relatively to the vehicle, the convective heat transfer coefficient is selected as 10 W/m²K.

To simulate the conduction heat transfer from the hot external air to the cool cabin air through the cabin surroundings, shell conduction with multiple layers is employed as a boundary condition in the solver. The materials used in the actual vehicle which has been used in the experiment was introduced to the solver and these materials and their actual thicknesses are allocated to the relative zones of the CFD model as illustrated in the Figure 21. Since the window consists of only one layer, wall thickness is employed in the window region.

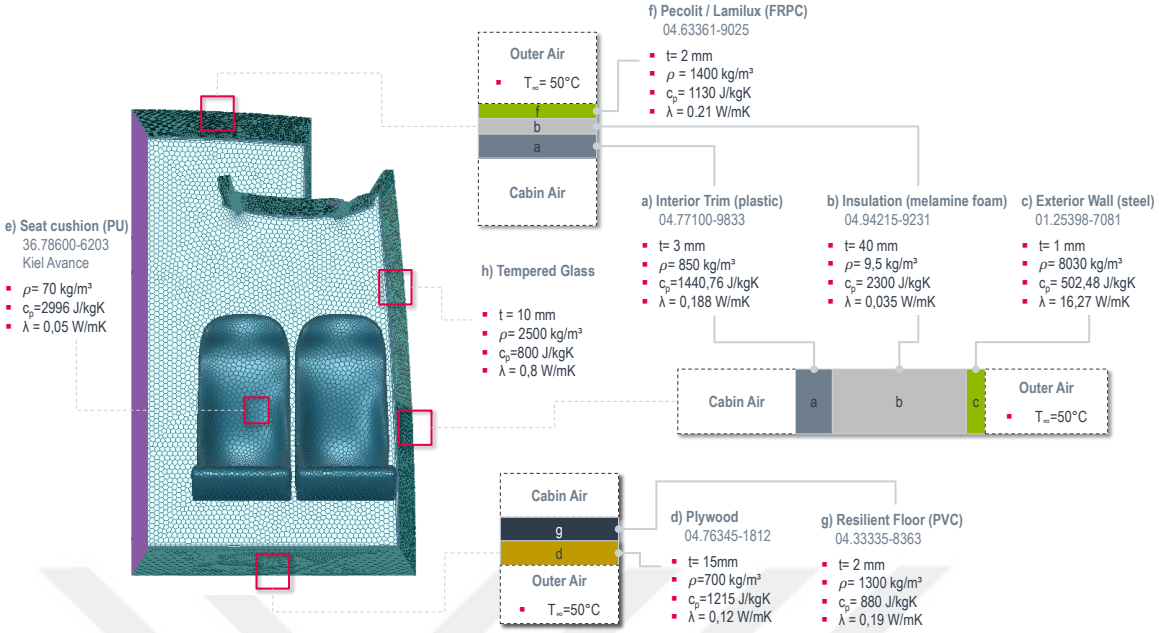

Figure 21. Conduction layers on the walls of the cabin

To capture the thermal effects of the buoyant forces inside the cabin, Boussinesq approximation, which is a proven method to simulate the buoyancy effect in the fluids with relatively low temperature differences, is employed. For gravity effects, gravitational acceleration is applied as -9,81 m/s² in the negative Y direction.

For the temperature boundary condition, the inlet temperatures obtained from the experimental methods with a time step of 0,1 seconds are introduced to the setup as a profile data. Since the CFD model only represents a section of the cabin which is periodic on the front and rear faces, the inlet temperatures measured from the middle section of the bus (8^{th} seat row) are introduced to the model as the temperature boundary condition For the only outlet, “pressure outlet” option is selected with the atmospheric pressure specified as 101.325 Pa.

2.3.4.5. Monitoring Points

Similar to the positions of the thermocouples used in the experimental methods, 3 monitoring points for each seat are created at the head, knee and foot levels. In order to plot

the temperature readings at those points over time, vertex average type report definitions are created and they are included in the output file.

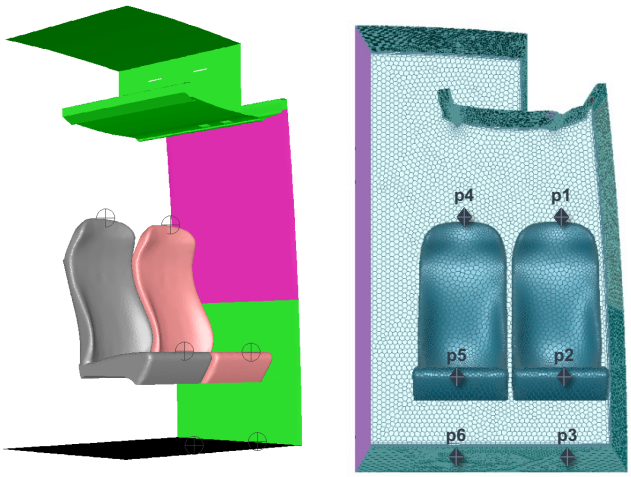

Figure 22. Positions of the monitoring points

2.3.4.6. Grid Independence Study

The two aspects that characterise an accurate and a successful simulation result are convergence and grid independence [20]. If the coarseness or fineness of the mesh effects the solution, then the solution is a function of the number of grids – an untenable situation. To overcome this dependency problem, the same analysis case is calculated using different meshes having different number of elements until reaching a solution which is no longer sensitive to the number of points [4].

In this study, 4 different mesh structures are generated having different number of elements by changing the curvature sizing controls, maximum cell length and growth rates of the cells. In order not to affect the nature of the flow from the inlets, the sizing controls in these regions kept the same in all variations. As a result, 4 different grid structures are obtained having different number of elements varying between 680k and 1,2 million (Table 6).

Table 6. Parameters used in the grid independence study

	Sizing Control	**Mesh 3.1.0 (finest)**	**Mesh 3.1.1**	**Mesh 3.1.2**	**Mesh 3.1.3 (coarsest)**
1	Curvature to all volume	1 -25 mm	1 -50 mm	1 -75 mm	1 -75 mm
2	Curvature to inlet & outlet edges	1 – 25 mm	1 – 25 mm	1 – 25 mm	1 – 25 mm
3	Proximity to inlet & outlet edges	0,5 – 25 mm 6 cells per gap	0,5 – 25 mm 6 cells per gap	0,5 – 25 mm 6 cells per gap	0,5 – 25 mm 6 cells per gap
4	Proximity to inlet & outlet faces	0,5 – 25 mm 6 cells per gap	0,5 – 25 mm 6 cells per gap	0,5 – 25 mm 6 cells per gap	0,5 – 25 mm 6 cells per gap
5	Boundary Layer	1st aspect ratio: 10 mm 5 layers	1st aspect ratio: 10 mm 5 layers	1st aspect ratio: 10 mm 5 layers	1st aspect ratio: 10 mm 5 layers
6	General Mesh Settings	Max cell length: 25 mm Growth rate: 1,10	Max cell length: 50 mm Growth rate: 1,10	Max cell length: 100 mm Growth rate: 1,15	Max cell length: 100 mm Growth rate: 1,20
	# of elements	1.209.644	1.066.970	813.165	681.759
	Max. skewness	0,79	0,81	0,75	0,75

The effect of the different sizing controls can be best observed in the bulk region, while the meshes around the inlets are more or less the same.

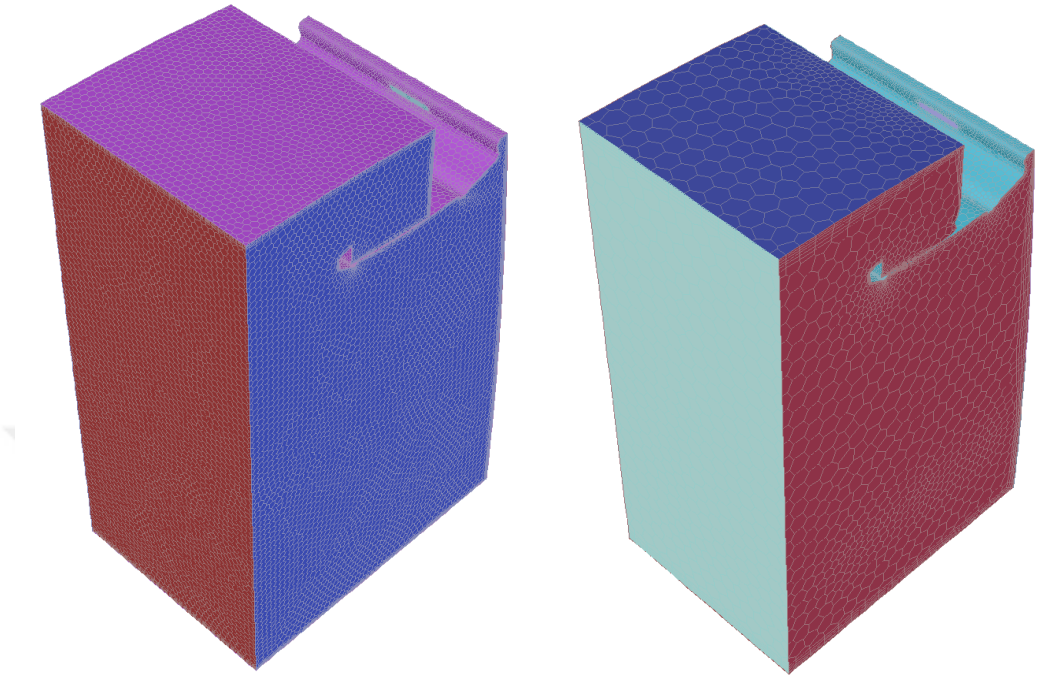

Figure 23. Finest (left) and coarsest (right) mesh models used in the grid independence study

In the grid independence study, the temperature values on the monitoring points are selected as the dependent variable. The results shown in Figure 24 outline that the solution using the coarsest mesh has shown a distinctive separation from the finer meshes, which proves that coarsest mesh is sensitive to the number of grid elements. On the other hand, the results obtained with the finer meshes, Mesh 3.1.0, 3.1.1 and 3.1.2 do not demonstrate a significant differentiation from each other, which makes Mesh 3.1.2 an optimum grid structure both in the means of reliability and calculation time for this CFD model.

Figure 24. Temperature readings in the grid independence study

3. FINDINGS AND DISCUSSION

The validation studies performed in scope of this thesis can be summarized in Table 7. In order to observe the effects of the materials and respective boundary conditions, the mesh models, the materials and the boundary conditions differ from each other while solver models and methods remain the same.

Table 7. Solver settings used in the validation study

	Transient 1	**Transient 2**	**Transient3**
Mesh	Mesh 3.0 (air volume only)	Mesh 3.1 (air volume + seats)	Mesh 3.1 (air volume + seats)
Materials	Air	Air + Seats	Air + Seats + Wall materials
Boundary Conditions	• Symmetry and periodicity • Temperature BC on inlets • Convection on window • Boussinesq for natural convection • Adiabatic walls	• Symmetry and periodicity • Temperature BC on inlets • Convection on window • Boussinesq for natural convection • Adiabatic walls • Coupled BC on seats	• Symmetry and periodicity • Temperature BC on inlets • Convection on window • Boussinesq for natural convection • Shell conduction on walls • Coupled BC on seats
Solver Model	pbns, rke-enhanced wall fn., transient, gravity: on	pbns, rke-enhanced wall fn., transient, gravity: on	pbns, rke-enhanced wall fn., transient, gravity: on
Methods	SIMPLE, 2nd Order PRESTO! On pressure Time step: 0,1 sec	SIMPLE, 2nd Order PRESTO! On pressure Time step: 0,1 sec	SIMPLE, 2nd Order PRESTO! On pressure Time step: 0,1 sec

‘Transient 1’ only includes air as the working material which is assigned to the cabin volume mesh with the hollow zones where the seats are located. After applying periodic and symmetry boundary conditions, inlet temperatures obtained from the experimental methods are introduced to the inlet faces as a function of time with a constant velocity of 1,7 m/s. The boundaries of the air volume is assumed perfectly isolated in the means of heat and mass transfer by assigning zero heat flux to those faces with the only exception of the window which a convective boundary condition is employed.

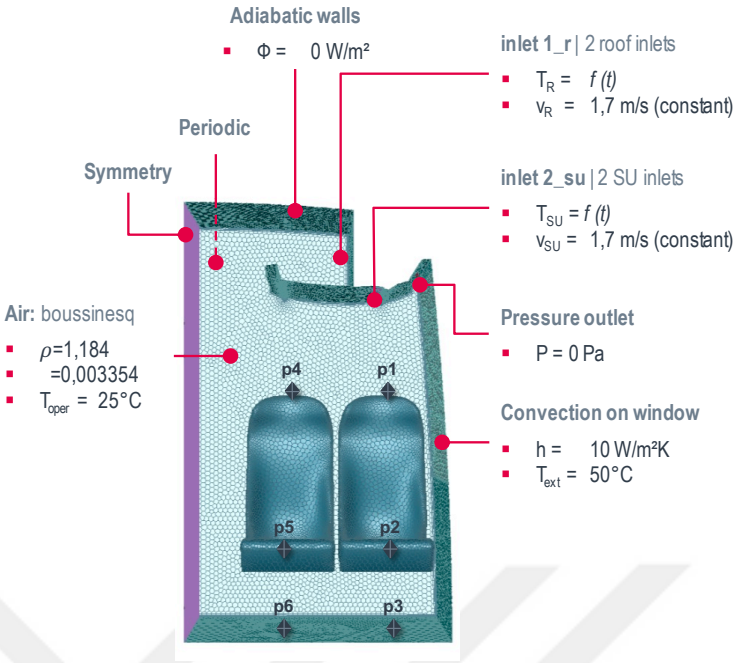

Figure 25. Boundary conditions of the solver setup ‘Transient 1’

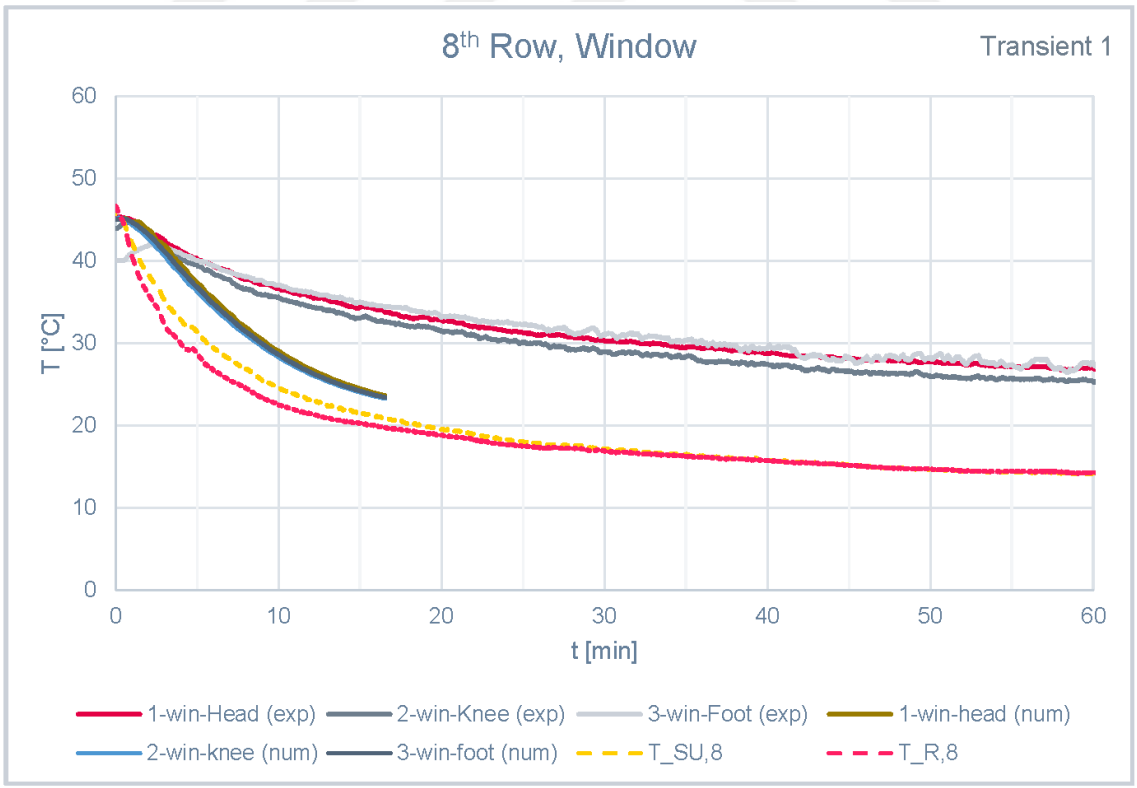

Figure 26. Results obtained from the solver setup 'Transient 1'

The results of the ‘Transient 1’ clearly indicate that the numerical solution is far from showing an agreement with the experimental measurements with a significant temperature difference of ~10°C. (Figure 26). Temperature differences between the head, knee and foot levels are very close to each other and they are trending to close the gap with the air inlet temperatures instead of experimental seat temperatures.

The constant gap between the inlet temperatures and experimental seat temperatures brings to mind that a constant amount of cooling power is lost by some means, which could be associated with the heat dissipation from the hot seats, or, the heat transfer from the hot external environment to the interior cabin air, or, a combination of these two phenomenon.

In order to take the heat absorbed by the seats into consideration in the ‘Transient 2’, the hollow zones in the first mesh model are filled with mesh elements and seat material is assigned to this zone. Similar to the boundary conditions in Transient 1, symmetry, periodicity, temperature BC on inlets, convection on window, boussinesq for natural convection and adiabatic walls are also employed. In addition, assigning a material to the seat zones enables Fluent solver to create coupled BCs on seat surfaces to simulate the heat dissipation from the seats to the cabin air (Figure 27).

The results of the ‘Transient 2’ indicate that simulating the seats in the CFD model contributes significantly to decrease the gap between the numerical and experimental results from ~10°C to ~5°C (Figure 28). Considering the initial temperature is 45°C at every point in the cabin at the beginning of the experiment, this result can be explained as the heat absorption effect of the seats, which also have the initial temperature of 45°C. Since the temperature readings at every point in the cabin is expected to reach an equilibrium in the long term, the seat material can absolutely be ignored for a steady-state condition, however, it is clearly observed that the transient effect of seat cooling has a significant importance in the validation of the CFD model, thus, it should be taken into consideration.

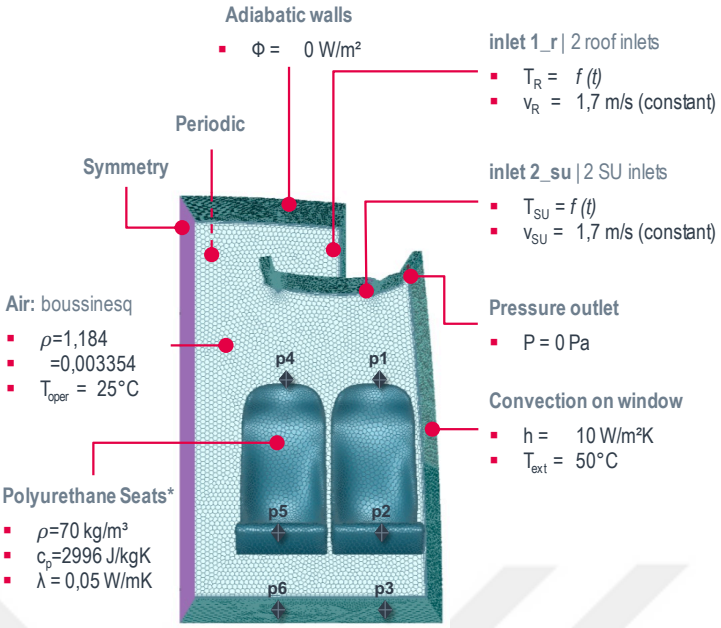

Figure 27. Boundary conditions of the solver setup ‘Transient 2’

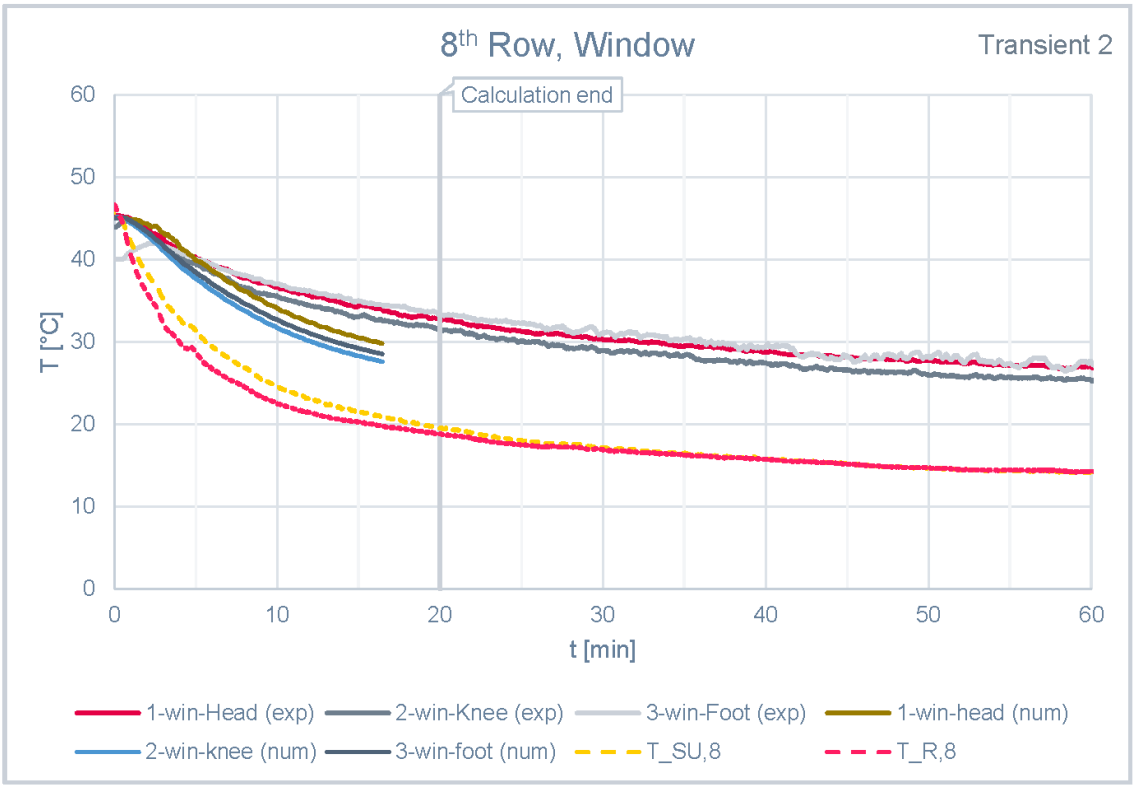

Figure 28. Results obtained from the solver setup 'Transient 2'

In order to reflect the experimental conditions perfectly into the analysis, heat transfer from the walls are also introduced to the CFD model. Therefore, a new setup solver 'Transient 3' is created with additional convective boundary conditions by introducing the materials at the roof, sidewall and floor surfaces as shown in the Figure 29.

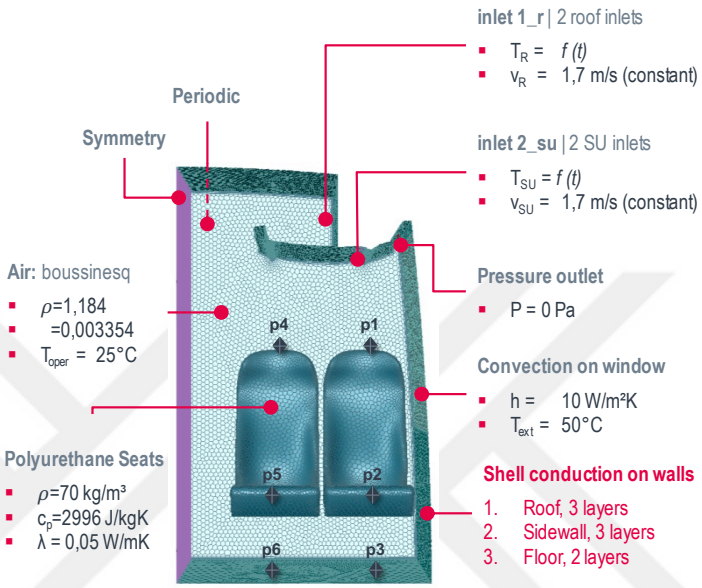

Figure 29. Boundary conditions for the solver setup 'Transient 3'

The results denote that the model with the combination of heat absorption effect of the seats with the convective heat transfer from the walls shows a good agreement with the experimental results (Figure 30). It can also be observed that the temperatures between the window and aisle seats does not exhibit a significant difference, similar to the experimental results (Figure 31).

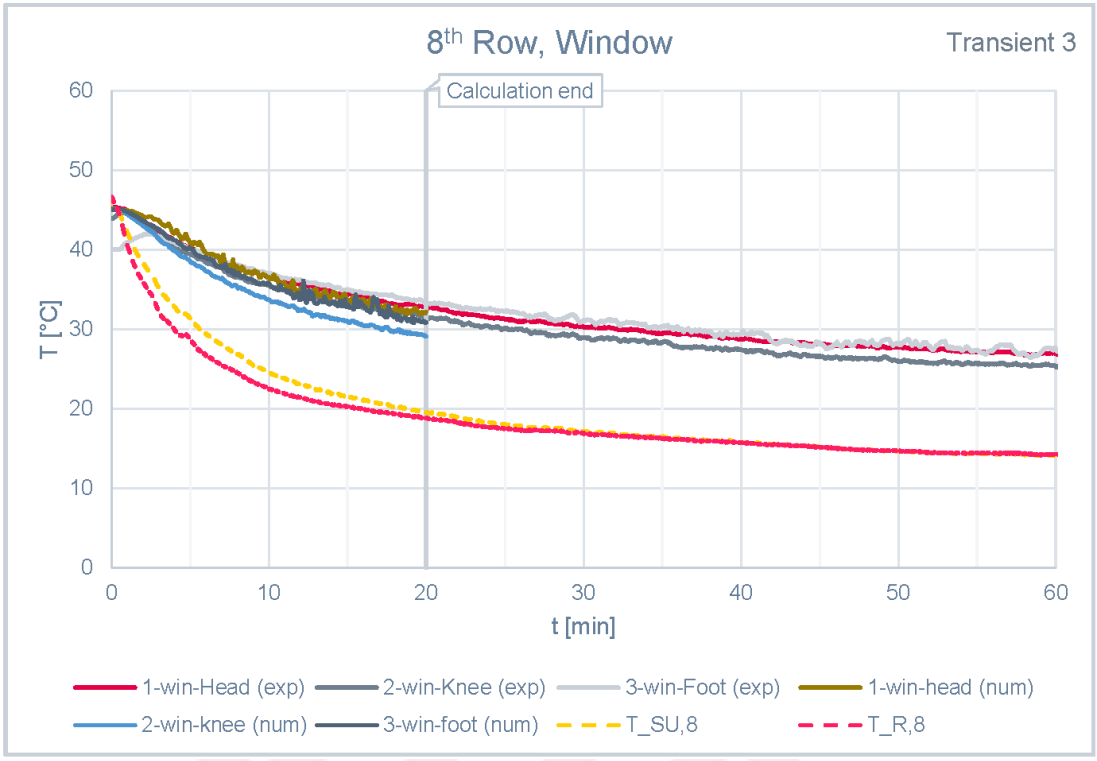

Figure 30. Results obtained from the solver setup 'Transient 3'

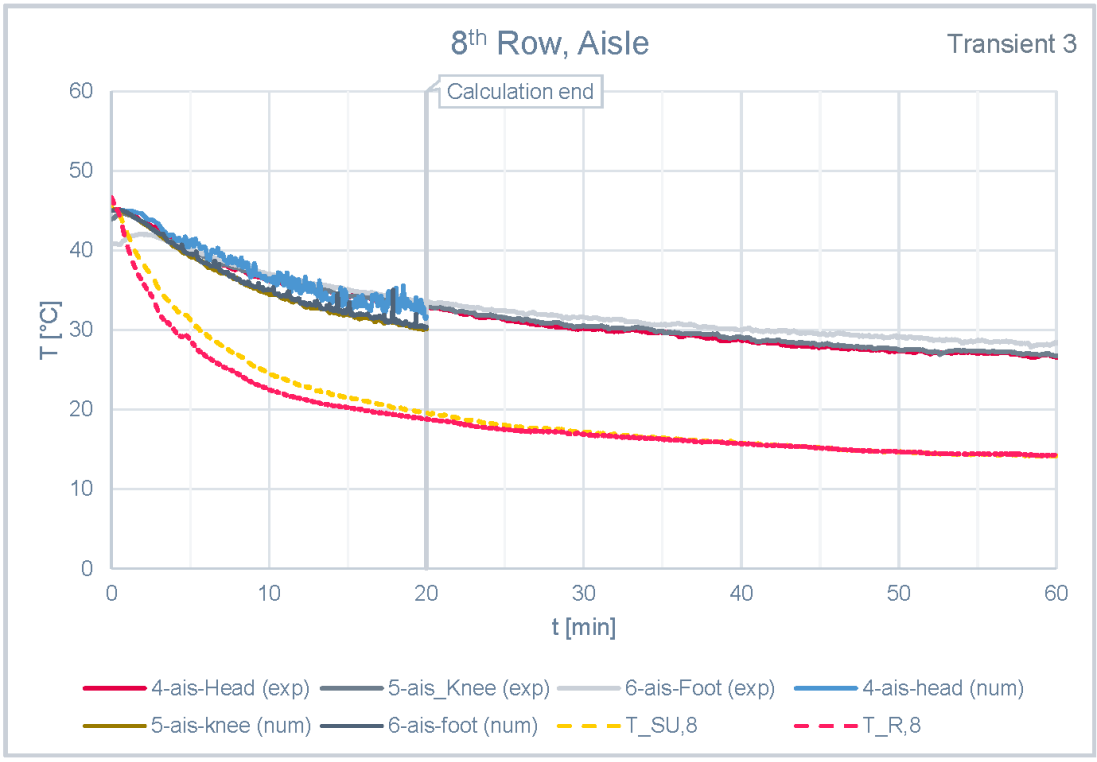

Figure 31. Results obtained from the solver setup 'Transient 3' (aisle)

Checking the model at the end of 20 minutes of the simulation (Figure 32), it can be seen that the wall temperatures vary between 18°C (inlet faces) to 47°C (window). Roof, floor and the window seems to have the highest temperatures, which also is an indication of high levels of heat transfer to the cabin interior. At that very instant, the air blown into the cabin at 18°C is only able to cool the seats around 30°C due to the excess heat dissipation from the seats and the heat fluxes from the walls heating up the cabin air.

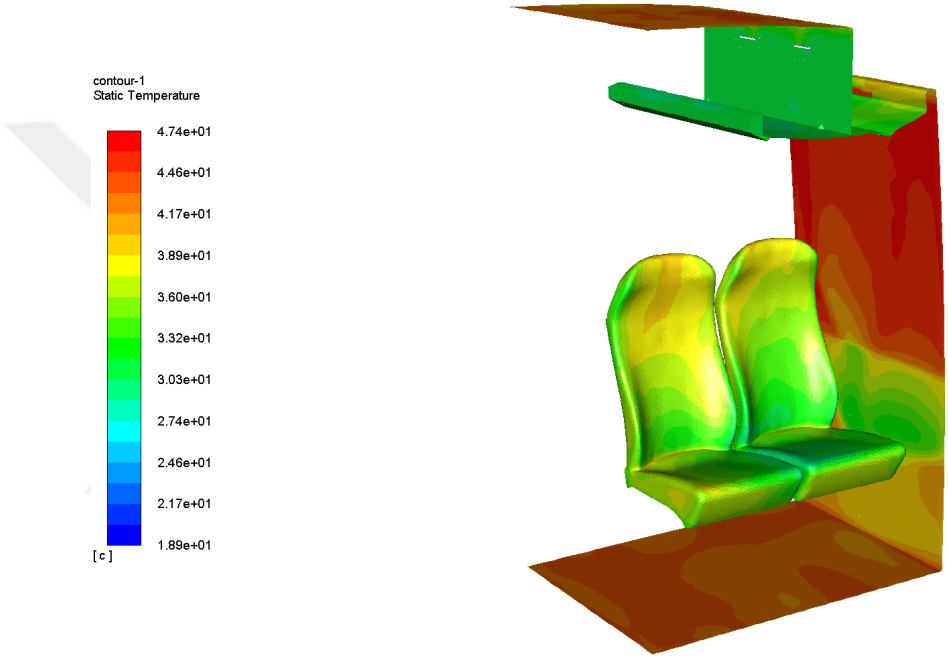

Figure 32. Wall temperatures at 20th minute in 'Transient 3'

It can be observed that the interior region of the seats still remain warm even after 20 minutes have passed (Figure 33). The temperature contour right above the headrest is indicating a significant region of the natural convection is dominant.

From the point of velocity and air mass, it could be stated that the window seat is been supplied with slightly higher rates of air. The service unit inlets are positioned right on the top of the window seat and has a slight design angle to the aisle seats. One can expect the window seat to be supplied with much greater amounts of air than the other, just because of the favourable positioning of the service unit inlets for the passenger sitting on the window seat. On the contrary, one can believe that the aisle seat is advantageous due to the design

angle of the inlet opening which faces directly to the headrest of the aisle seat. The simulation shows the design angle of the service unit inlet performs a great coherence with the air supplied from the roof inlets and reflected from the symmetry plane causing the air blown from the service unit to change direction and to head towards the area between the seats providing a relatively homogeneous distribution between window and aisle seats (Figure 34).

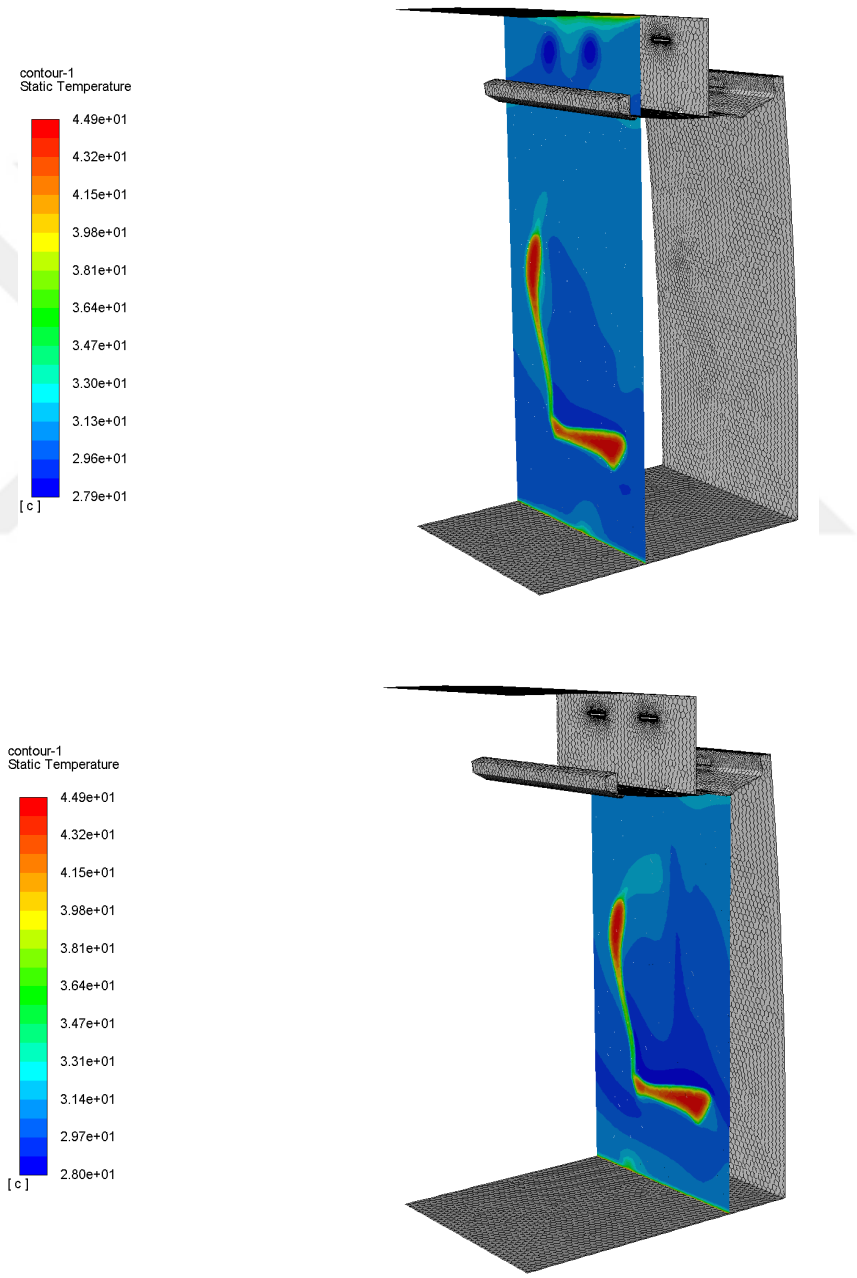

Figure 33. Temperature contours of 'Transient 3'

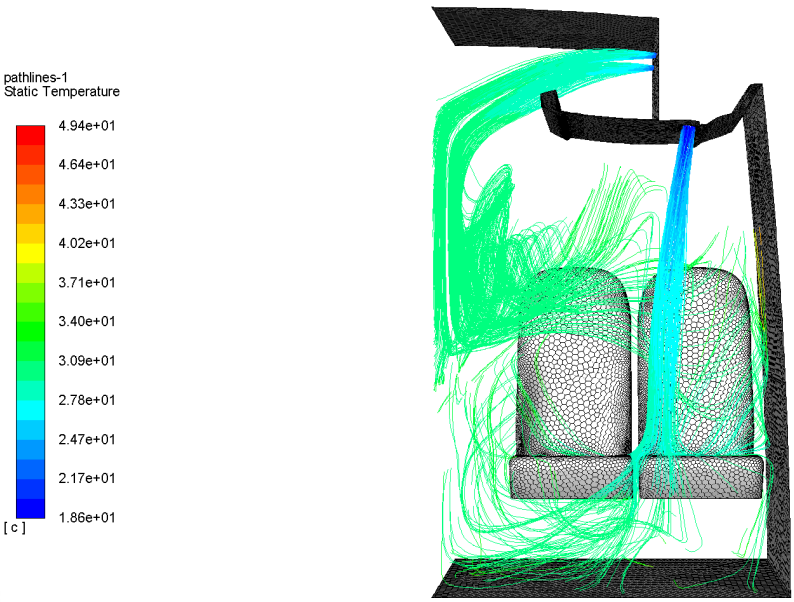

Figure 34. Path lines of the air blown into the cabin, Transient 3

4. CONCLUSIONS

1. A detailed experimental dataset of a cooling process of a bus cabin is obtained which might be further used as input parameters for any further CFD validation of a similar type of bus cabin.
2. A validated CFD model of a specific bus cabin is obtained which can be utilized for further thermal investigation of the same vehicle type with lesser experimental needs.
3. It has clearly observed that the validation of a CFD model strongly depends on the accuracy of the geometry, the quality of the mesh model, selection of the appropriate solver setup, preciseness of the material properties and correctness of boundary conditions assigned.
4. The heat absorption and heat dissipation phenomena of the materials inside the cabin might not be of crucial importance in steady-state conditions, but it is proven to have a strong effect in a transient analysis. In this study, the heat absorption of the seats is significantly dominated the validation of the CFD model by decreasing the temperature difference between the experimental and numerical methods from ~10°C to ~5°C The materials used in the cabin interior can also be taken into consideration in the future.
5. Consideration of heat transfer through the walls also played a crucial role in the analysis and makes the numerical results identical with the experimental results. It can be stated that the temperature difference between the cabin with adiabatic walls and the cabin with layered walls showing realistic conductivity properties denotes the energy loss due to the isolation issues.
6. In the transient cooling analysis of a CFD model of a bus cabin, a combination of the material properties of the solids and the walls must be taken into consideration with relevant and reasonable boundary conditions.

5. FUTURE WORKS

The literature review proves that, in the past decade, there is a considerable interest in wall bounded flow simulations, particularly in the air and temperature distribution inside vehicle cabins. It can also be stated that these studies mostly focused on increasing passenger comfort and increasing cabin air quality by contamination removal from the passenger compartments, which according to my personal belief, might not be of a short term interest to many of the commercial enterprises. I believe that focusing more on commercial research that may lead to a direct commercial benefit (fuel efficiency, energy savings and etc.) has a greater potential on catching the interest of the commercial companies, utilization of the innovative research outputs and yet receiving a possible research funding which provides the sustainability of a continuous "research – benefit – research" cycle.

Further research on innovative methods on vehicle air-conditioning which yield fuel efficiency might be of interest for the willing researchers. Zonal cooling, which can be utilized according to the passenger density or solar load intensity, is a promising field of research that may result with energy savings for a wide range of commercial vehicles. Personalized cooling, on the other hand, is an another field of research that might be of interest for the narrower audience, like high-end vehicle manufacturers whose customers are willing to pay more for additional comfort.

The effects of different isolation materials in different thicknesses or the combination of different layers of materials can also be observed using this validated CFD model. By doing so, a preliminary insight could be obtained on the isolation effects of alternative isolating material combinations without undertaking the burden of prototyping or testing costs.

Modelling the whole bus can also be considered as a topic for further research, since the luggage compartment in long distance buses acts like a natural isolation during the journey and such analysis with a whole bus model will surely yield different results. In a similar manner, temperature distribution in city buses which does not have a luggage compartment and having a massive heat source –the engine– positioned right beside the passengers sitting on the rear seats could also be investigated.

It can be recommended to the future researchers who are willing to conduct a similar study to perform a climatic chamber experiment with a set of pre-determined test conditions

including heating and cooling of the cabin under extreme conditions, to collect temperature and velocity readings from many different points inside the cabin, to consider collecting ‘mass flow rates’ from the inlets instead of air velocities and to continue the test until all the readings reach a steady state, which provides the researcher the option to validate the model in steady state conditions in the CFD analysis which might be very profitable in the means of calculation times.

6. REFERENCES

1. https://www.fueleconomy.gov/feg/atv.shtml U.S. Department of Energy, Office of Energy Efficiency - Where the Energy Goes: Gasoline Vehicles. 24 April 2019.

2. Yenneti, S., Punuru, P. and Nayak, G., Optimization of a Main Engine Driven RoofTop Bus Air-Conditioning System, 15th International Refrigeration and Air Conditioning Conference, Indiana, July 2014, 2510-2520.

3. Weilenmann, M.F., Alvarez, R. and Keller, M., Fuel Consumption and CO^2 Pollutant Emissions of Mobile Air Conditioning at Fleet Level-New Data and Model Comparison, Environmental Science and Technology, 44 (2010) 5277-5282.

4. Anderson J.D., Computational Fluid Dynamics: The Basics with Applications, McGraw-Hill, New York, 1995.

5. Arıcı, Ö., Yang, S., Huang, D. and Öker, E., Computer Model for Automobile Climate Control System Simulation and Application, International Journal of Applied Thermodynamics, 2 (1999) 59-68.

6. Shah, R.K., Automotive Air-Conditioning Systems - Historical Developments, The State of Technology and Future Trends, 3rd BSME-ASME International Conference on Thermal Engineering, December 2006, Dhaka, 720-735.

7. ANSI/ASHRAE 55-2004, Thermal Environmental Conditions for Human Occupancy, ASHRAE, Atlanta, 2004.

8. Zhang, H & Huizenga, C & Arens, Edward & Yu, T., Modeling thermal comfort in stratified environment, Indoor Air 2005, 2005, Beijing, 133-137.

9. Güney, G., Air Flow and Temperature Distribution Analysis in a Coach Bus Cabin, MSc. Thesis, Hacettepe University, Graduate School of Science and Engineering, Ankara, 2016.

10. Sevilgen, G., Otomobil Kabininde Hız ve Sıcaklık Dağılımının Üç Boyutlu Sayısal Analizi, PhD Thesis, Uludağ University, Institute of Applied Sciences, Bursa, 2010.

11. Doğan, B., Bir Taşıt İçindeki Havalandırma/Isıtma (Isıl Dağılım) Probleminin Sayısal Olarak İncelenmesi, MSc. Thesis, Yıldız Technical University, Institute of Applied Sciences, İstanbul, 2011.

12. Şahin, D., Analysis of Flow Structure in a Helicopter Cabin to Improve the Thermal Comfort Using Computational Fluid Dynamics Modeling, MSc. Thesis, METU, Graduate School of Natural and Applied Sciences, Ankara, 2018.

13. Paulke, S., Artmeier, F. Yıldırım, K.E., Bader, V. and Gübner, A., MAN Bus A37: HVAC Analysis & Benchmark with THESEUS-FE, Project Report, Munich, 2013.

14. Zhu, S., Demokritou, P. and Spengler, J., Experimental and numerical investigation of micro-environmental conditions in public transportation buses, Building and Environment, 45 (2010) 2077-2088.

15. Yıldırım K.E., Ercan, A., Bader, V. und Gores, I., Beurteilung und Optimierungsmöglichkeiten der Kabinentemperatur und Insassenbehaglichkeit durch Messungen mit IR-Kameras, 7. VDI-Fachkonferenz Thermomanagement in elektromotorisch angetriebenen PKW, November 2018, Stuttgart.

16. Pala, Ü., Investigation of Thermal Comfort Parameters in Bus Design, PhD Thesis, Fatih University, Graduate School of Sciences and Engineering, İstanbul, 2014.

17. You, R., Zhang, Y., Zhao, X., Lin, C., Wei, D., Liu , J. and Chen, Q., An innovative personalized displacement ventilation system for airliner cabins, Building and Environment, 137 (2018) 41-50.

18. Dehne, T., Lange, P., Volkmann, A., Schmeling, D., Konstantinov, M. and Bosbach, J., Vertical ventilation concepts for future passenger cars, Building and Environment, 129 (2018) 142-153.

19. Petrone, G., Fichera, G. and Scionti, M., Thermal and Fluid-dynamical Optimisation of Passengers Comfort in a Touring Bus Cabin, COMSOL Conference, 2008, Hannover.

20. Versteeg, H. K. and Malalasekera, W., An Introduction to Computational Fluid Dynamics, 2nd Edition, Pearson Education Limited, Glasgow, 2007.

21. ANSYS, Inc., ANSYS Fluent Theory Guide, Release 15.0, Canonsburg, 2013

22. ANSYS, Inc., ANSYS Fluent User's Guide, Release 15.0, Canonsburg, 2013.

23. Ekici, Ö., and Güney, G., Experimental and Numerical Investigations of Heating in a Bus Cabin under Transient State Conditions, WIT Transactions on Engineering Sciences, Vol 118 (2017) 49-59.

24. ANSYS Inc., Database of ANSYS Fluent 19.2 Computational Fluid Dynamics Software, 2018.

25. Kolich M., Dooge, D., Doroudian, M., Litovsky, E., Ng, R. and Kleiman, J., Thermophysical Properties Measurement of Interior Car Materials vs. Temperature and Mechanical Compression, SAE International Journal, vol. 7, no. 3 (2014) 646-647.

26. Pau, D. S. W., Fleischmann, C. M., Spearpoint, M. J. and Li, K. Y., Thermophysical properties of polyurethane foams and their melts, Fire and Materials, vol. 38 (2014) 433-450.

27. Ashby, M. F., Materials and the Environment, 2nd Edition, Elsevier Inc., London, 2012.

28. MAN Truck & Bus AG, Technical Datasheet of Melamine Insulation (Part Nr. 04.94215-9231), Ankara, 2013.

29. https://www.engineering.com/Library/ArticlesPage/tabid/85/ArticleID/152/Thermal-Conductivity.aspx Engineering.com Portal, 25 April 2019.

30. https://www.altro.co.uk/Support/Technical-documents/Technical-data-sheets Altro Corporate Website, 15 April 2019.

31. https://www.engineeringtoolbox.com/specific-heat-polymers-d_1862.html The Engineering Toolbox, 25 April 2019.

32. https://www.lamilux.de/downloads.html Lamilux Composites GmbH, 25 April 2019.

33. https://ctherm.com/products/tci_thermal_conductivity/helpful_links_tools/thermal_physical_properties_conductivity_effusivity_heat_capacity_density2 C-Therm Technologies Website, 24 April 2019.

34. https://www.saint-gobain-sekurit.com/glossary/automotive-glazing Saint - Gobain Main Website, 24 April 2019.

RESUME

Zeki Mert Barut born in 1984 in Ankara. After receiving his Bachelor of Science degree in Mechanical Engineering from Karadeniz Technical University in 2008, he has gained experience as a Mechanical Design Engineer in PROKAL A.Ş. and worked as a Technology & EU Projects Expert in Trabzon Chamber of Commerce and Industry for 5 years. Currently working as a Senior Expert in the R&D Centre of MAN Truck & Bus Ankara Plant since 2014, Zeki Mert Barut engages in project planning, research funding and university-industry collaboration, experienced in R&D and innovation management and intellectual property rights and aims to build up a career on science and become competent in the field of computational fluid dynamics. He also enjoys practicing bass sessions, preparing Italian coffee and caring his ’74 Volkswagen Beetle. He speaks good English and German and a little Italian.